FACULDADE DE ENGENHARIA DA UNIVERSIDADE DO PORTO

INSTITUTO DE CIÊNCIAS BIOMÉDICAS ABEL SALAZAR

Development of functional gut-on-chip epithelial models to study intestinal absorption

Ana Cristina da Rocha Miranda

Master in Bioengineer – Molecular Bioengineer

Work developed at:

Under the supervision of **Miguel Xavier, PhD**

University of Porto co-supervisor: **Professor Bruno Sarmento, PhD**

October, 2022

This dissertation was supervised by:

Miguel Xavier, PhD

International Iberian Nanotechnology Laboratory

Food Processing and Nutrition Research Group

Professor Bruno Sarmento, PhD

Institute for Research and Innovation in Health, University of Porto

Nanomedicines & Translational Drug Delivery Research Group

The host institution of this dissertation was:

INL - International Iberian Nanotechnology Laboratory, Avenida Mestre José Veiga, 4715-330 Braga, Portugal.

The research described in this dissertation was financially supported by:

MICRODIGEST project (grant agreement 037716) co-funded by FCT and ERDF through COMPETE2020.

European Union's Horizon 2020 research and innovation programme through the project GASTRIC, under the Marie Sklodowska-Curie grant agreement no. 101003440.

SbDToolBox project (NORTE-01-0145-FEDER-000047), supported by Norte Portugal Regional Operational Programme (NORTE 2020), under the PORTUGAL 2020 Partnership Agreement, through the European Regional Development Fund (ERDF).

© Ana Miranda, 2022

Development of functional gut-on-chip epithelial models to study intestinal absorption

Ana Cristina da Rocha Miranda

Master in Bioengineer – Molecular Bioengineer

October 14, 2022

Resumo

Culturas celulares estabelecidas em modelos bidimensionais (2D) pecam frequentemente pela incapacidade de simular tecidos humanos nativos, em particular aqueles com arquitecturas tão distintas como é o caso do intestino. O desenvolvimento de modelos *in vitro* com propriedades biomiméticas optimizadas é fundamental para reforçar a relevância fisiológica destes sistemas e alcançar estudos mais precisos sobre condições e patologias humanas mais complexas. Os dispositivos de microfluídica são vistos como potenciais novas plataformas para estudos *in vitro* que permitirão ultrapassar algumas limitações dos modelos estáticos convencionais.

Os estudos de bioacessibilidade e biodisponibilidade são importantes para determinar a eficácia e segurança de novos medicamentos e formulações alimentares. Os modelos baseados em células são normalmente utilizados para estudar a absorção intestinal. As culturas celulares 2D são geralmente fáceis de utilizar, apresentam um bom custo-benefício e não impõem muitas preocupações éticas, ao contrário dos modelos animais. No entanto, a maioria das culturas celulares não permite mimetizar a estrutura tridimensional (3D) do intestino humano, o que limita a sua relevância fisiológica. As tecnologias de organoides surgiram como uma alternativa, ao fornecerem um microambiente 3D, apesar de não contemplarem a dinâmica caracteristica intestino. *Organs-on-chip* são dispositivos microfluídicos que permitem a integração de múltiplos parâmetros celulares e fisiológicos do tecido *in vivo*, facilitando uma representação mais precisa da fisiologia humana.

Co-culturas Caco-2 e HT29-MTX foram integradas em dispositivos de microfluídica sob fluxo contínuo de meio de cultura – *gut-chip* - (cultura dinâmica) e em *cell culture inserts* (cultura estática), como experiências de controlo para a investigação futura envolvendo cultura de células intestinais primárias no mesmo dispositivo. É apresentada uma breve comparação entre os modelos estáticos e dinâmicos. Para validar o *gut-chip* , foi realizado um ensaio funcional com base na atividade da glicoproteína P (P-gp) em ambos os modelos. Resultados preliminares mostraram que a atividade da P-gp poderia ser utilizada para comprovar a relevância fisiológica dos modelos, no entanto, devem ser realizadas experiências adicionais.

Células intertinais primárias foram isoladas de amostras de tecido intestinal humano, proveniente de intestino delgado ou de colon, para avaliar a presença e morfologia das criptas intestinais. As criptas isoladas foram cultivadas para o desenvolvimento de organoides intestinais. Foram obtidas estruturas semelhantes a organoides, embora não tenha sido possível manter subculturas viáveis.

Palavras-chave: modelos 3D *in vitro*, modelos celulares, *gut-on-a-chip*, absorção intestinal, glicoproteína P, permeabilidade aparente

Abstract

Cell cultures within two-dimensional layouts often fail to mimic native human tissues, particularly those with such distinctive architectures as is the case of the intestine. The development of *in vitro* models with improved biomimetic properties is key to strengthen the physiological relevance of these experiments and achieve more accurate studies of complex human diseases. Microfluidic chips are viewed as potential new platforms for *in vitro* studies that can overcome some limitations of conventional static models.

Bioaccessibility and bioavailability studies are important to determine the effectiveness and safety of novel medicines and food formulations. Cell-based models are commonly used to study intestinal absorption. 2D cell cultures are usually easy to use, present a good cost-benefit and do not impose many ethical concerns, in contrast to animal models. However, most cell cultures fail to represent the three-dimensional aspect of the human intestine, which limits the physiological relevance of these models. Organoid technologies emerged as an alternative, by providing a 3D microenvironment, nevertheless disregarding flow dynamics in the gut. Organ-on-chip are microfluidic devices that enable the integration of multiple cellular and physiological parameters of the *in vivo* tissue, facilitating a more precise representation of human physiology.

Caco-2 and HT29-MTX co-cultures were established in microfluidic gut-chip devices (dynamic culture) and cell culture inserts (static culture), as control experiments for further research involving culture of primary intestinal cells on-chip. A brief comparison between the static and dynamic models is presented. To validate the gut-chip, a P-glycoprotein functional assay was conducted on both models. Preliminary results showed that P-gp activity could be used to prove physiological relevance of the models, however additional experiments must be conducted.

Primary intestinal cells were isolated from human small intestine or colon samples to assess the presence and structural morphology of intestinal crypts. Isolated crypts were cultured for the development of primary intestinal organoids. Organoid-like structures were obtained, even though it was not possible to maintain viable subcultures.

Keywords: 3D *in vitro* models, cell-based models, microfluidics, gut-on-a-chip, intestinal absorption, P-glycoprotein, apparent permeability

Para as minhas pessoas e os meus lugares.

Acknowledgements

This work would not be possible without many people to whom I am deeply grateful and will try to not forget to mention herein.

First of all, my supervisor, Miguel Xavier for his important guidance and extensive feedback during the whole work. Professor Bruno Sarmento to whom I am thankful for promptly accepting to be co-supervisor. Catarina Gonçalves for giving me the opportunity to be a part of this project since day 1.

I am deeply grateful for the constant collaboration and the warmest welcome of my colleagues from Food Processing and Nutrition Group.

Patrícia and Mafalda, my unofficial supervisors, thank you for teaching me I should make loads of mistakes in order to learn more and do better. *Mommy*, I am deeply grateful for all your support and the great moments of dancing and singing that we shared (hopefully, no one was watching!). I am an admire of your strength and dedication, the world should have more people like you. Mafalda, thank you for your eternal patience and guidance. Vitor *The Aligner* Calero, for being the worst post-doc ever (!!) and all the laughs, *aunque eres muy "pesá"*! Helena, thank you for helping me with everything, (literally) covering my back since (your) day 1. It was great having you to rely on, while listen to great Portuguese Indie music.

Marisolzita, for appreciating all my "potinhos" and being the sweetest good morning. Rui, for sharing good music and always having the right thing to say. Pedro, for all the unwanted advice that I didn't realize I needed and for helping me even when it was not your place to. To all my colleagues at Food Processing and Nutrition Group, I am grateful for their warm welcome, all the sweets and cakes (no wonder I gained weight!).

To INL, the city and the people of Braga for always making me feel like home.

João Meneses, I am grateful for your support during my whole stay at INL, literally taking me there. Ana Martins, this last few months would have been way more difficult without your permanent cheerfulness around the lab, thank you for your constant encouragement.

Catarina, Nuno, Ricardo e Bruno thank you for being there for me over the last 5 years. All of these would be much more sad without you guys and our musical adventures.

To my greatest friends Helena, Nela, Inês, Rita e Filipa who supported me for the last 6 years. I know it wasn't always easy, but you always made it easier for me to continue.

NEBianos do meu coração, you guys completed my path by constantly and effortlessly moving me out of my comfort zone. I am thankful for the time we had.

Sara and Iolanda my oldest and dearest friends, thank you for always being there for me, even miles apart.

“Everything will be okay in the end.
If it’s not okay, it’s not the end.”

Indian Proverb, John Lennon, Paulo Coelho or maybe Fernando Sabino

x

Table of Contents

List of figures

List of abbreviations and notations

ABC	ATP-superfamily of transporters
AF488	Alexa Fluor™ 488
AF647	Alexa Fluor™ 647
ATP	adenosine triphosphate
BCRP	Breast Cancer-Resistant Protein
CD	Chron's Disease
CNC	Computer Numerical Control
CYP3A4)	Cytocrome P450 3A4
DMEM	Dulbecco's Modified Eagle Medium
DMSO	Dimethyl Sulfoxide
DTT	Dithiothreitol
EDTA	Ethylenediaminetetraacetic Acid
FBS	Foetal Bovine Serum
GIT	Gastrointestinal tract
HBSS	Hanks' Balanced Salt Solution
HEPES	4-(2-hydroxyethyl)-1-piperazineethanesulfonic acid
HIO	Human Intestinal Organoids
HIOs	Human Intestinal Organoids
IBD	Inflammatory Bowel Disease
iPSCs	Induced Pluripotent Stem Cells
KCl	Potassium Chloride
KH2PO4	Potassium Dihydrogen Phosphate
MEM	Minimum Essential Medium
Na2HPO4	Disodium Hydrogen Phosphate
NaCl	Sodium Chloride
NGS	Normal Goat Serum
PBS	Phosphate Buffered Saline
PDMS	Polydimethylsiloxane
PMMA	Poly(methyl 2-methylpropenoate)
PTFE	Polytetrafluoroethylene
Rho123	Rhodamine 123
rpm	rotations per minute
RT	Room Temperature
SBS	Short Bowel Syndrome
Sulfo-SANPAH	Sulfosuccinimidyl 6-(4'-azido-2'-nitrophenylamino)hexanoate
TEER	Transepithelial Electrical Resistance
UC	Ulcerative Colitis
VRP	Verapamil hydrochloride

Chapter I

Work outline

1. Framework

Even though conventional two-dimensional (2D) *in vitro* intestinal models are frequently used by the pharmaceutical industry, e.g., for pharmacokinetic (PK) and pharmacodynamic (PD) studies, these models often fail to replicate the human intestinal physiology – in particular, its three-dimensional (3D) aspect, which is crucial for cellular-matrix interconnections and subsequent tissue morphology of the gut. (Ashammakhi et al., 2020; Bein et al., 2018). Moreover, these models are typically static and therefore do not allow the co-culture of commensal microorganisms, a fundamental feature of normal gut physiology, due to rapid bacterial overgrowth (Bein et al., 2018; Kim et al., 2012).

Animal models recapitulate the 3D structure and dynamic complexity of the native organ. However, animal responses to certain treatments are often inconsistent with what happens in humans. Besides, these models are expensive and raise ethical concerns (Ashammakhi et al., 2020).

Aiming to bridge the gap between 2D *in vitro* systems and *in vivo* models, intestinal 3D organoid cultures have been used. Even though organoids may be able to give rise to different types of intestinal cells, their structures hinder the presence of other important supporting cells, such as muscle cells. Furthermore, these models are still ineffective to represent the mechanical aspects of the intestine, due to the absence of its distinctive peristaltic movements and fluid flow (Bein et al., 2018). Bearing all this in mind, it is essential to extend the development and implementation of dynamic models, encompassing other structural and mechanical properties that can fully recapitulate vital aspects of the native intestinal tissue.

Current progress in the field of microfluidics and microfabrication enabled the establishment of integrated systems, coined organ-on-a-chip, which provide a specialized microenvironment that facilitates a more precise representation of human physiology (Ashammakhi et al., 2020; Bhatia & Ingber, 2014). These microengineered chips encompass major advantages, including the simultaneous monitoring of multiple parameters, as well as easy adjustments to the whole system environment. Moreover, organ-chips can integrate fluid dynamics and mechanical cues (Bhatia & Ingber, 2014; Workman et al., 2018). Thus, Organ Chip systems are considered a good solution to surpass previous biological models, granting clearer knowledge about human pathologies and possible treatments (Beaurivage et al., 2020).

2. Objectives

The present work is integrated in the MICRODIGEST and GASTRIC projects, which coincide in their main objective to fabricate a modular microdevice to mimic the complete gastrointestinal tract to predict the digestibility, bioaccessibility and bioavailability of orally ingested bioactive compounds.

The present work aimed to validate the cell-based gut-chip device as a model to study intestinal absorption. Moreover, human intestinal colon samples were used to obtain primary cells to establish organoids cultures to be used in the microdevices. To accomplish this, the following specific objectives were established:

- Establishment of a functional gut-chip model;
- Validation of the gut-chip model using a P-glycoprotein (P-gp) inhibition assay, and comparison with standard 2D models (cell culture inserts);
- Isolation and expansion of primary intestinal organoid cultures.

3. Dissertation outline

This dissertation is divided in seven chapters and an appendix.

Chapter I (Work outline) provides an overview of the project, comprising an introductory note to the overall background, objectives, and structure of the dissertation.

Chapter II (Introduction) introduces the theoretical context to this work. The human gastrointestinal tract is described, with primary focus on the small intestine epithelium, cell types and functions, and the process of intestinal absorption. Active transport is emphasized with the introduction of P-glycoprotein as a key player in this

mechanism. The importance of gut epithelium experimental models is stressed by their potential to aid the development of new therapeutic approaches.

Chapter III (Materials and Methods) describes the materials and methods used throughout the project including device microfabrication, cell seeding and expansion, methodologies to evaluate cell barrier integrity, and a functional assay targeting the activity of p-glycoprotein.

Chapter IV (Results and Discussion) presents the results obtained during this works, followed by their corresponding discussion. This chapter includes confocal microscopy images of the cultures, monolayer integrity assessment, apparent permeability coefficient measurements and efflux ratio, and optical images of the isolated intestinal crypts and the resulting organoid cultures.

Chapter V (Conclusions) concludes the dissertation by recapitulating the overall results and discussion, presenting some suggestions to future work.

Chapter II

Introduction

1. Gut anatomy and physiology

Orally ingested food products and drugs are processed along the gastrointestinal tract (GIT), which extends from the oral cavity to the anus. Along this route, substances flow through the organs of the GIT, including the oesophagus, stomach, small and large intestines, each performing specific functions within the GIT. In fact, these organs work together with the pancreas, liver, and gall bladder to complete the processes of digestion and absorption, leading to effective nutrient uptake by the human body. Intestinal absorption is crucial to complete this process allowing the delivery of bioactive compounds into the bloodstream (Diehl et al., 2020; Thompson et al., 2018).

Among all GIT organs, the small intestine is where most drug molecules and food nutrients are absorbed (Diehl et al., 2020). This long duct of about 3 to 5 m in length is divided into 3 functional regions: duodenum, jejunum, and ileum. Each segment of the small intestine has specific functions. The epithelial cells of the duodenum synthesize digestive enzymes that, together with bile and pancreatic enzymes, complete the digestion of proteins, fats, and carbohydrates. Nutrient absorption takes place mostly in the jejunal epithelium. Finally, vitamin B12 and bile salts are absorbed in the ileum (Thompson et al., 2018). Moreover, the ileum contains a great variety of bacteria populations, Peyer's patches, and is where most goblet cells reside (Diehl et al., 2020; Dubé, 2020). Recognizing the different characteristics of each region in the small intestine epithelium is key to understand the development of diseases associated with loss of epithelium integrity. For instance, pathologies such as Short Bowel

Syndrome (SBS), IBD or Colorectal Cancer. Consequently, this knowledge gives rise to new potential therapies (Thompson et al., 2018).

The distinctive architecture of the small intestine lumen is critical to proper intestinal function. In fact, the available surface area determines absorption capacity of this organ. Thus, even though the epithelium is mainly composed of simple columnar shaped cells, the mucosal surface area is augmented due to its distinctive cellular arrangement into finger-like projections, the villi, and the formation of invaginations, the intestinal crypts (Dubé, 2020; Thompson et al., 2018).

Villi are composed of enterocytes, intercalated with goblet cells and M cells (**Figure 1**). Enterocytes function as absorptive epithelial cells and are the most numerous cell type in the villi (Diehl et al., 2020). Intestinal crypts are located at the bottom of the villi and are composed of crypt cells, which are secretory cells. Crypt cells are intestinal stem cells that can give rise to differentiated cells including absorptive epithelial cells and cells from the secretory lineage (Diehl et al., 2020). The secretory cell lineage is essentially composed of goblet cells, enteroendocrine cells, tuft cells, and Paneth cells. Goblet cells make up approximately 10% of the intestinal epithelium and are responsible for producing and secreting mucus. The mucous layer protects the absorptive epithelial cells from microorganisms and toxins. Besides, it functions as a passive diffusion interface for drug molecules before they reach epithelial cells. Enteroendocrine cells regulate cell processes by secreting hormones into the *lamina propria*. Tuft cells secrete opioids to control pain, gastric emptying, intestinal secretion, and gut motility. Finally, Paneth cells secrete antimicrobial peptides into the lumen (Diehl et al., 2020; Dubé, 2020).

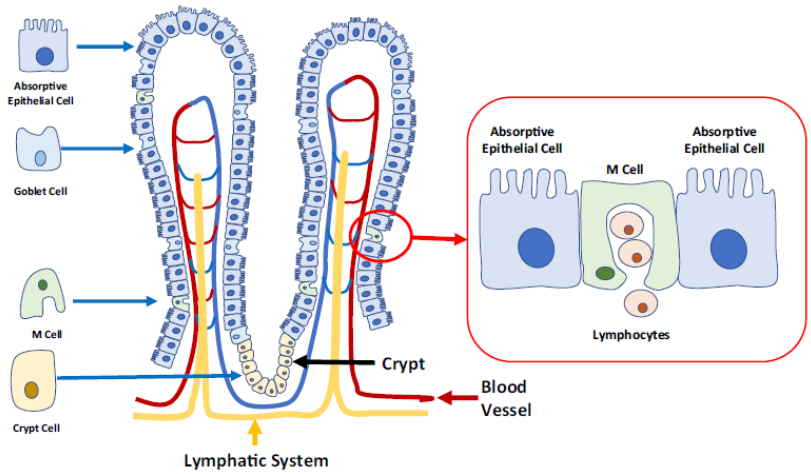

Figure 1 *- The structure of the small intestine villi, composed of absorptive epithelial, Microfold (M), goblet, and crypt cells. The crypt region at the bottom of villi is populated with crypt cells (Diehl et al., 2020).*

2. Bioaccessibility and bioavailability in orally administrated compounds

The concepts of bioaccessibility and bioavailability are often described as synonyms, when in fact they are related to distinct stages of the gastrointestinal processes. Bioaccessibility encompasses all the transformations of a compound throughout digestion until it reaches the colon, representing the portion that becomes available in the body for intestinal absorption. Bioavailability, in its turn, is the fraction of ingested food or pharmacological compound that reaches systemic circulation, following intestinal absorption and first-pass metabolism, and becomes available for physiological processes, storage or to exert a therapeutic effect on the target site. (Fernández-García et al., 2009; Langerholc et al., 2011).

Bioaccessibility and bioavailability can be assessed by *in vivo* studies, such as balance and bioassay studies, and using *in vitro* models, which can be static or dynamic. *In vitro* digestion studies are used to determine the influence of digestion (peristaltic movements, pH, enzymatic activity) or interactions with other food components, since these may affect the efficacy of bioactive compounds. Intestinal absorption can be evaluated using *in vivo* and *ex vivo* models or cell culture-based approaches (Fernández-García et al., 2009).

2.1. Mechanisms of crossing the intestinal mucosal layer

Drug and food bioavailability in the intestine is highly influenced by the presence of multiple metabolizing enzymes and transporter proteins. Enzymes act as metabolic barriers at the intestinal epithelium, by converting proteins and carbohydrates into nutrients, as well as degrading toxic molecules and inhibiting their passage to the systemic circulation. On the other hand, transporter proteins can prevent the crossing of several molecules from the cell membranes of the intestinal mucosa. Their activity is similar to multidrug-resistant proteins, which block the entrance of anticancer drugs into tumour cells (Diehl et al., 2020).

Intestinal absorption of any molecule implies its permeation through the intestinal epithelium, typically via absorptive epithelial cells. This process may occur via passive or active transcellular and/or paracellular transport mechanisms, or by carrier-mediated transport, which can also be either active or passive (**Figure 2**) (Anderle et al., 2004; Steffansen et al., 2004).

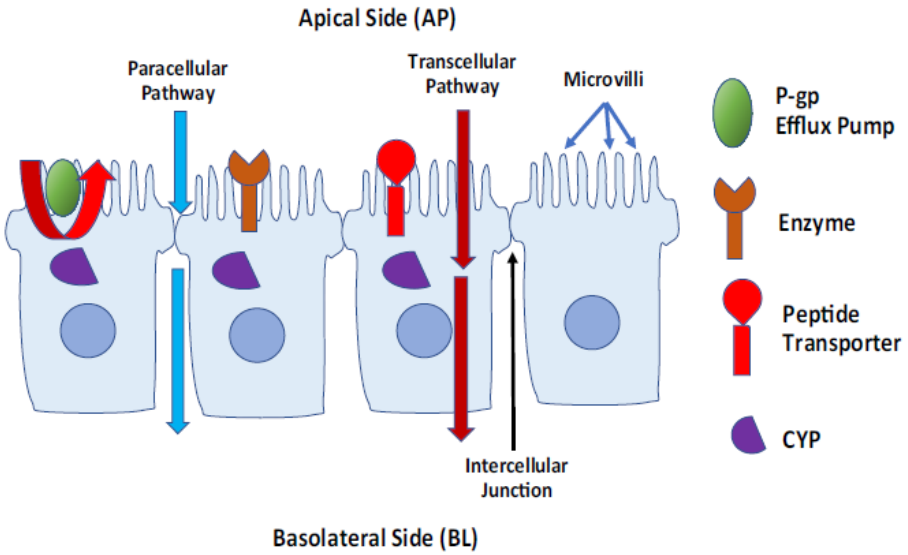

Figure 2 *- The general structure of absorptive epithelial cells with microvilli or brush borders that are decorated with P-gp efflux pump, peptidase enzymes, and transporters The transport of drug molecules through the intestinal mucosa from the lumen to the blood side can utilize transcellular and paracellular pathways. (Diehl et al., 2020).*

Passive, transcellular diffusion of molecules occurs within individual cells and can be influenced by transporter proteins present in their membrane. Most hydrophobic molecules cross the intestinal mucosal barrier by passive diffusion. The paracellular route refers to the passage of molecules between two distinct cells, by crossing their tight junctions, and is restricted to smaller hydrophilic molecules and ions (Diehl et al., 2020; Laksitorini et al., 2014).

Carrier-mediated transport is established by proteins embedded in the cellular membrane. These membrane proteins create an electrochemical gradient across cell membranes and allow the transport of polar and positively charged molecules, such as amino acids, dipeptides, organic cations, phosphates, water-soluble vitamins, and others. Based on their transport mechanism, they can be classified as channels or carriers. Carriers are subdivided into facilitated diffusion, primary and secondary active transporters, depending on whether their function requires energy or not. Facilitated diffusion results from the establishment of an electrochemical concentration gradient and enables membrane crossing with the aid of uniporters (membrane transport proteins). Primary and secondary active transports are distinguished by the source of energy used. The first implies ATP hydrolysis into ADP, with subsequent energy release due to the rupture of a highly energetic phosphate bond. ATP-powered pumps such as F-, P- and ABC-type ATPases are examples of primary active transporters. In the case of secondary active transport, the energy stems from ion gradients generated by primary active ion pumps as is the case of the Na^{+}/Ca^{2+} ATPase (Anderle et al., 2004).

2.2. P-glycoprotein as the model efflux pump

P-glycoprotein (P-gp) was one of the first transporter proteins to be discovered (Juliano & Ling, 1976) and it has been the most widely studied efflux protein for over 45 years (Frances Jane Sharom, 2014). P-gp is part of the adenosine triphosphate (ATP) binding cassette (ABC) superfamily of transporters, subfamily B (ABCB). This protein pumps substrates out of cells through an ATP-dependent mechanism, which protects the tissues against potentially harmful substances. However, P-gp is also a key contributor to the occurrence of multidrug resistance in many therapies, including cancer chemotherapy. Along with multidrug resistance-associated proteins (MRPs), and breast cancer-resistant protein (BCRP), P-gp integrates the multidrug-resistant (MDR) transporters family (Abdallah et al., 2015; Diehl et al., 2020; Martins et al., 2019).

Human P-gp is encoded by two MDR genes, MDR1/ABCB1, and its size ranges from 140 to 190 kDa, according to different glycosylation levels. Although P-gp expression levels are low in most human tissues, it prevails in epithelia with transport functions, such as the colon, small intestine, liver, pancreas, kidneys, uterus and placenta, and in the blood-brain barrier (Abdallah et al., 2015; Martins et al., 2019).

P-gp concentrations are higher on the apical surface of the intestinal epithelium, where the protein is embedded in the cell membrane of absorptive epithelial cells. The level of expression also varies with age and gender, which results in drug absorption variability among individuals (Diehl et al., 2020; Martins et al., 2019).

2.2.1. Mechanisms of action

In general, P-gp substrates are amphipathic, hydrophobic, and nonpolar molecules. These compounds range from natural products, chemotherapeutic drugs, steroids, linear and cyclic peptides to fluorescent dyes and ionophores. Thus, there is a wide variety of molecules that interact with this protein and are prone to be effluxed out of cells. This phenomenon is important to protect certain tissues from harmful molecules, however it impairs intracellular drug bioavailability of many therapeutic agents (Martins et al., 2019; Frances J. Sharom, 2011).

There are essentially two hypotheses to the P-gp transporters mechanism of action: the “hydrophobic vacuum cleaner” and the “flippase” mechanism (**Figure 3**). Both models were proposed by Gottesman and Higgins, in 1992 (Higgins & Gottesman, 1992). The first model suggests that hydrophobic substrates are embedded in the plasma membranes, where they gain access to the P-gp binding pocket and are then effluxed

to the extracellular space, throughout the protein channel. The “flippase” mechanism relates to the flipping motion of the substrate induced by the efflux pump. After entering the cell, P-gp substrates intercalate with the lipids from the cytoplasmatic membrane. Subsequently, the substrates interact with the transmembrane part of the efflux protein which leads P-gp to “flip” the molecules into the outer lipid layer. From then on, substrate molecules start accumulating in the outer leaflet and a concentration gradient is created, which results in their diffusion into the extracellular space (Diehl et al., 2020; Frances Jane Sharom, 2014).

2.2.2. P-glycoprotein inhibitors as chemosensitizer agents

P-gp inhibitors are molecules that diminish the protein ATPase activity and transport (Seelig, 2020). Cyclosporines, alkaloids, coronary vasodilators, quinolines, hormones, calcium channel blockers and many surfactants are some examples. Molecules such as Verapamil, valinomycin, cyclosporin A, quinidine, and LY335979s inhibit P-gp activities, which increases intestinal drug absorption. Many components of products of plant origin also influence drug absorption due to inhibition of P-gp, as is the case of different seeds, roots and plant leaves (Abdallah et al., 2015; Diehl et al., 2020). Thus, there is an opportunity to explore the potential of these molecules as a way of enhancing oral bioavailability of drugs and other bioactive compounds. Verapamil (VRP) is part of the first generation of P-gp blockers, along with other calcium channel blockers and non-blockers. This molecule is considered the P-gp prototype blocker, it has strong inhibiting activity and is known to improve intracellular delivery of anticancer drugs (Abdallah et al., 2015). However, Verapamil administration imposes cardiac implications and serious immunosupressive effects. Similar consequences were

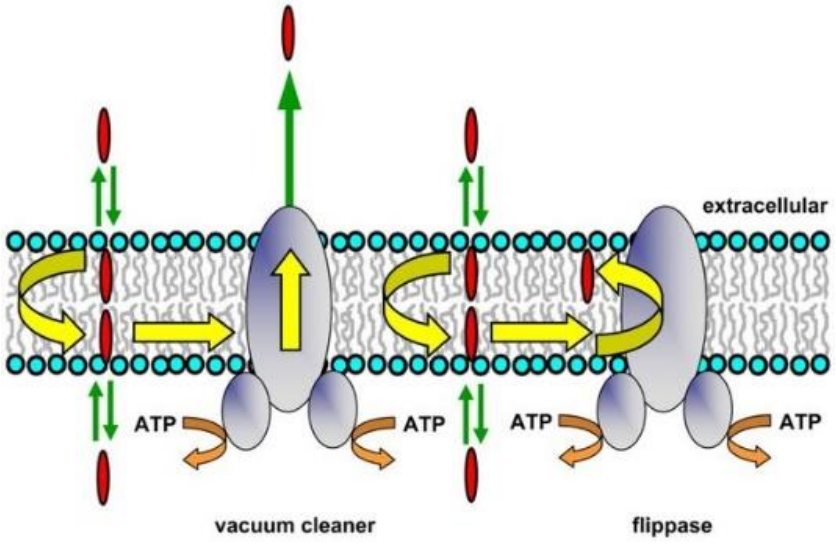

***Figure 3** – The “hydrophobic vacuum cleaner” and “flippase” mechanism proposed by Gottesman and Higgins in 1992 (Frances J. Sharom, 2011).*

denoted by the use of Cyclosporin-A, the most frequently used immunosuppresive agent. Moreover, research has verified that most of these compounds only exert their effects at concentrations much higher than their therapeutic windows, becoming toxic to patients. Second generation P-gp blockers emerged in the quest for dimminished cellular toxicity and higher selectivity. This led to the synthesis of structurally equivalent compounds. These molecules were considered more efficient and imposed less collateral effects. Among these, dexverapamil, the R-isomer of VRP with no cardiac effects, and PSC 833, an equivalent to Cyclosporin-A lacking immunosupressive functions (Abdallah et al., 2015; G. Lee et al., 2018). Even with decreased toxicity, second generation blockers could not be used clinically since most also inhibited cytocrome P450 3A4 (CYP3A4) (G. Lee et al., 2018), a crucial metabolyzing enzyme of the intestine. Finally, third generation inhibitors were developed to tackle the aforementioned limitations, by combining structural and chemical modifications. The aim was to obtain the least cytotoxic effects and residual interactions with other anticancer drugs. Further investigation and clinical trials are still in progress (Abdallah et al., 2015; G. Lee et al., 2018).

As an alternative, P-gp inhibitors of natural origin have been studied (Ampasavate et al., 2010; Choi et al., 1998; Hu et al., 2014; G. Lee et al., 2018; Lu et al., 2013). These include naturally occurring compounds such as flavonoids, stilbenes, coumarins, terpenoids, alkaloids and saponins (Abdallah et al., 2015). Among other plant-based products, tea and fruit juices are beverages consumed daily around the world (Tamura & Matsui, 2000). Research shows that tea contains thousands of bioactive compounds, the majority of which are polyphenols. Polyphenols are a large group of plant chemicals that includes flavonoids and catechins (Carsalade et al., 2012). These compounds can modulate ABC transporters responsible for cancer drug resistance, including P-glycoprotein. Flavonoids and stilbenes are known to produce comparable effects to Verapamil and Cyclosporine (Abdallah et al., 2015). Catechins are responsible for other health benefits attributed to tea, in particular green tea. The most active and abundant catechin in green tea is epigallocatechin-3-gallate (EGCG), a flavonoid also reported as a P-gp inhibitor (Abdallah et al., 2015; Carsalade et al., 2012). Green tea is obtained from the tea plant *Camellia sinensis* and is usually associated to other health benefits, such as anticarcinogenic, antioxidative and anti-aging activities (Carsalade et al., 2012; Zhang et al., 2006).

3. *In vitro* intestinal models

Over the years, many different experimental systems have been developed to recapitulate different aspects of the intestinal epithelium, including *ex vivo*, *in vitro,* and *in vivo* models. These models are of utmost importance to assess the intestinal absorption of pharmaceutical and nutritional products prior to human consumption. (Rahman et al., 2021; Westerhout et al., 2014).

Characterized as a highly dynamic and complex tissue, the intestinal epithelium comprises a highly diverse cellular content and it is the fastest renewing tissue of the body, with a distinctive 3D architecture and mechanical properties (Ashammakhi et al., 2020; Creff et al., 2021). Consequently, the predictive value of current systems is frequently diminished regarding the overall complexity of the human GIT (Westerhout et al., 2014). In fact, the unique topographic and mechanical characteristics of the intestine are crucial features for many of the organ functions and strongly influence the correct differentiation and proliferation of the cells it harbours (Creff et al., 2021). Therefore, the development of physiologically relevant biomimetic systems of the human intestine must include a specific architecture into which appropriate cell sources are incorporated and provided with proper mechanical cues (Ashammakhi et al., 2020). Moreover, it is particularly important to consider the interplay between active transport and metabolism, as potential food-drug and excipient-drug interactions (Westerhout et al., 2014).

3.1. Cancer-derived epithelial cell lines

Cell lines derived from colorectal cancers, such as HT-29, Caco-2, T84, or SW480, are the most commonly used cell sources for *in vitro* studies of the intestinal epithelium, due to their ease of access and high proliferation rate (Creff et al., 2020). Caco-2 cells were first isolated by Fogh and Trempe (Fogh & Trempe, 1975) from a human colorectal adenocarcinoma and are used for most experiments concerning drug adsorption and permeability, or even differentiation assays (Creff et al., 2021). These cells exhibit enterocyte-like characteristics following spontaneous differentiation *in vitro*, including the formation of a polarized cell monolayer with apical and basolateral membranes. Moreover, Caco-2 cells present apical brush borders with prominent microvilli, and express tight junctions' proteins and many enzymes and transporters that are typically associated with native enterocytes (Creff et al., 2021; Shim et al., 2017). In addition, they have been shown to be able to form villi structures in a spontaneous manner (Kim & Ingber, 2013). Therefore, these cells are widely used to

model intestinal absorption and transport, as well as to conduct bioavailability assays, since they also express important metabolising enzymes such as CYP3A4 (Pelkonen et al., 2001; Ponce de León-Rodríguez et al., 2019). However, Caco-2 cells are unable to produce a mucous layer, which is crucial to study molecule permeability given that it affects solubility over the cell surface (Ashammakhi et al., 2020), and fail to represent cell heterogeneity, a distinctive feature of the native intestinal tissue (Beaurivage et al., 2020; Creff et al., 2021).

To tackle these limitations, co-cultures with other cell types have been the subject of extensive studies. Goblet cells, for instance, were previously integrated to enhance the production of mucus (Béduneau et al., 2014); and immune cells, in their turn, were used to assess possible immunological reactions within the tissue (Ramadan & Jing, 2016). Additionally, other mechanical cues have been incorporated into the cell cultures, which increased the expression of metabolic enzymes, mucus proteins and the development of villi-like structures (Kim et al., 2012; Kim & Ingber, 2013).

The HT-29 cell line also established by Fogh and Trempe (Fogh & Trempe, 1975), resembles some of the key characteristics of Caco-2 cells as an enterocyte model. The HT29-MTX clone, a methotrexate (MTX)-resistant population of HT-29, exhibits spontaneous differentiation into goblet-like mucus-producing cells, adding physiological relevance to cell-based intestinal models (Lesuffleur et al., 1990; Ponce de León-Rodríguez et al., 2019; Verhoeckx et al., 2015). Caco-2 and HT29-MTX are frequently utilised in co-culture for intestinal absorption studies, as it has been demonstrated that integrating both cell lines results in a more physiologically relevant model to analyse drug permeability *in vitro* (Hilgendorf et al., 2000; Lozoya-Agullo et al., 2017).

3.2. Primary Cells, Stem Cells & Organoid Cultures

The establishment of a reproducible protocol to isolate and expand viable human intestinal epithelium *in vitro* (Sato et al., 2009, 2011) enabled the development of *in vitro* models that mimic the *in vivo* physiology of the tissue. In fact, primary epithelial cells can be incorporated into several types of *in vitro* systems, from organoid cultures, monolayer systems, or three-dimensional engineered systems. Each system recapitulates important aspects of the intestinal physiology, such as the architectural arrangement of the tissue, constant fluid flow, and other mechanical cues such as peristaltic movements. This was made possible with the introduction of chemical gradients or physical forces across the tissues (Dutton et al., 2019).

In contrast to cancer-derived cell models, primary intestinal cells cultures will likely include all the intestinal epithelial subtypes, corresponding receptors, transporter proteins, and other metabolizing enzymes at similar levels to the ones *in vivo*. These advances in primary cell culture gave rise to increasingly sophisticated experimental systems which provide useful insights about gut microbiota's impact on intestinal homeostasis, and the progress of common inflammatory diseases of the intestine, such as IBD (Dutton et al., 2019).

Organoids can be obtained either from human biopsies (Kasendra et al., 2018, 2020) or from induced pluripotent stem cells (iPSCs) (Beaurivage et al., 2020; Workman et al., 2018). Regardless of the origin, human intestinal organoids (HIOs) typically show polarization, are prone to be kept in a highly controlled environment for a long time, and their cellular content should include all four cell types found in the native intestinal epithelium (Workman et al., 2018). In addition, HIOs hold self-renewing and self-organizing capacities, recapitulating these distinct properties of the original tissue. However, the shape and dimensions of HIOs in culture are very diverse, and it is particularly difficult to access the lumen, which hinders the analysis of essential intestinal parameters, such as permeability, microbiome interactions, and drug absorption. Moreover, these culture systems are usually integrated into three-dimensional matrices, which impair the seeding of other cells from the immune system or even vascular cells (Creff et al., 2021; Workman et al., 2018). Thus, communication among neighbouring cells is very scarce in HIOs, diminishing the physiological relevance of these models (Beaurivage et al., 2020).

Kasendra et al. (Kasendra et al., 2018) developed a primary human small intestine chip, combining intestinal organoids (or enteroids) and organ-on-chip technology. The system included epithelial cells obtained from individual patient biopsy-derived enteroids and intestine-specific endothelial cells. This Intestine Chip is viewed as a representative model of the native duodenum microenvironment since it closely replicates crucial elements of the tissue physiology. These included the formation of three-dimensional structures resembling the original gut villi, and a polarized epithelium within which multi-lineage differentiation markers of the 4 main cell subtypes found in the native intestinal epithelium (enterocytes, goblet cells, enteroendocrine cells, and Paneth cells) were expressed, as well as basal proliferative cells. Moreover, the model showed enzymatic activity and mucus production and allowed for continuous access to the fluids flowing across the apical lumen.

3.3. Microfluidic Gut-on-Chip

Current progress in the field of microfluidics and microfabrication enabled the establishment of integrated systems, coined organ-on-a-chip, which provide a specialized microenvironment that facilitates a more precise representation of human physiology (Ashammakhi et al., 2020; Bhatia & Ingber, 2014). These microengineered chips encompass major advantages, including the capacity for simultaneous monitoring of multiple parameters, as well as easy adjustments on the whole system environment (Bhatia & Ingber, 2014; Workman et al., 2018). Thus, Organ Chip systems are considered a good solution to surpass previous biological models, granting clearer knowledge about human pathologies and possible treatments (Beaurivage et al., 2020).

Typical gut-on-a-chip devices consist of two main chambers separated by an epithelial-like tissue, which grows on top of a microporous membrane, thus replicating the natural intestinal barrier. This membrane is usually made of a polymer which is then coated with extracellular matrix (ECM) components (Bein et al., 2018). On the other chamber, endothelial cells can be cultured aiming to replicate the vascular endothelium. Other components can be incorporated in these microengineered systems, including sensors, electrodes and valves. The addition of further cellular or synthetic elements contributes to the establishment of an efficient replica of a functional gut, emulating its natural chemical, biological and mechanical features (Ashammakhi et al., 2020). A schematic representation of a gut-on-a-chip device and variations of different components can be found in **Figure 4**.

Kim and Ingber (Kim & Ingber, 2013) demonstrated that Caco-2 cells could undergo villus morphogenesis when exposed to appropriate physiological and mechanical signals, such as peristaltic-like movements and circulating fluid flow. Moreover, these

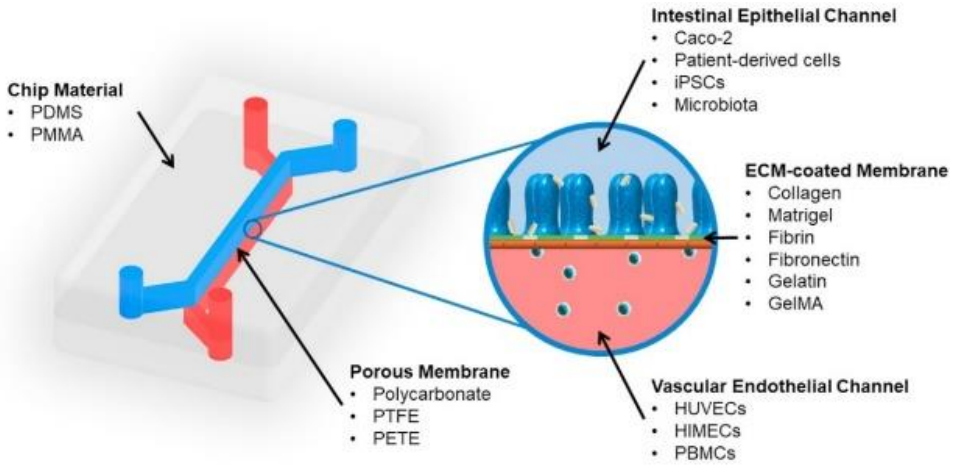

***Figure 4** - Schematic representation of a microfluidic gut-on-chip device (Adapted from Ashammakhi et al., 2018).*

structural changes in the morphology of cell cultures stimulate the manifestation of other biomimetic characteristics of the native tissue. In fact, villi architecture promotes the extension of the intestinal surface area, as well as improved metabolic activity, namely of CYP3A4 enzyme. This accentuates the importance of the *in vitro* microenvironment in the development of physiologically relevant models.

Similarly, Shim et al. (Shim et al., 2017) studied the possibility of stimulating additional alterations in Caco-2 cell physiology by associating two key aspects of the native human intestine: its 3D structure and the shear stress induced by fluid circulation. This was assessed by comparing the resulting tissue morphology and cell functions among 3 different culture conditions: 2D monolayers on Transwells® and microfluidic chips, and 3D-scaffold cultures on microfluidic chips. The authors observed a significant reduction in the height of the villi when Caco-2 cells were cultured on the 3D scaffold, which was hypothesized as a consequence of increased exposure to contraction under those conditions. Cell morphology was considered similarly good in both 2D and 3D cultures, denoting only slight differences, for instance a more prismatic appearance on the latter. This experiment further validated previous studies concerning the improvement of CYP450 3A4 activity when cell cultures were exposed to fluid dynamics and a 3D topography.

3.3.1. Host-microbiome interaction and disease modeling

The GIT harbours 10^{14} microbes, including viruses, archaea and eukarya, along with the major resident bacteria. Thus, it comes as no surprise that this is where most of the immune system-microbiome crosstalk occurs. Any alteration in the composition of the gut microbiota significantly impacts the intestinal equilibrium, many times eliciting dysbiosis with consequent development of inflammatory diseases (Bäckhed et al., 2005; Round & Mazmanian, 2009).

Inflammatory bowel diseases , such as Crohn's disease and ulcerative colitis, are some of the chronic inflammatory conditions affecting the intestine. The pathology of IBD is commonly characterized by the inability to maintain a structurally sound intestinal epithelium, which favours the free movement of the microbiota through the gut tissue. The presence of these microorganisms in atypical locations elicits an exacerbated inflammatory response, with increased immunological infiltration and consequent intestinal damage. In contrast to what happens in a healthy individual, some immunological regulatory mechanisms are absent in IBD patients. Thus, they are not capable of controlling inflammation through the usual recruitment of immune cells to the mucosa, resulting in a persistent inflammatory state (Beaurivage et al., 2020).

There are many parameters related to inflammatory intestinal diseases that cannot be controlled in an independent manner when using animal or *in vitro* models, such as mucosal injury and villus destruction, suppression of peristalsis, and the gut interaction with its microbiome. Intestinal microbiota, in particular, have been recently identified as a key factor in human pathology. Thereby, it urges the need to include commensal bacteria in experimental assays, currently not achievable when using standard culture methods (Kim et al., 2016).

Several studies have tried to reproduce gut-microbiota interactions, including conventional cell culture inserts systems and organoid cultures (Dutta & Clevers, 2017; Fatehullah et al., 2016; Sadabad et al., 2015). However, co-culturing human epithelial cells and living microbes within these models is usually not sustainable for more than one day, mainly due to exceeding bacterial growth and consequent cell death. In addition, it is particularly challenging to maintain low oxygen levels in organoid cultures, which is an essential parameter for the survival of some anaerobic microbes (Bein et al., 2018; Williamson et al., 2018).

Kim et al. (Kim et al., 2012) described a gut-on-a-chip where they integrated a strain of *Lactobacillus rhamnosus* GG (LGG). LGG cells were cultured separately and then placed above Caco-2 cells monolayers, which were previously grown in one of the chambers of the microfluidic system. This procedure was replicated in static cultures, using cell culture inserts as experimental controls. When under continuous flow and cyclic strain for 96 hours, LGG colonies remained adhered to the Caco-2 cell monolayer. Caco-2 cell viability was also maintained, as well as intestinal barrier function which was enhanced in the presence of the bacteria. However, under static conditions, barrier integrity decreased, and the epithelial monolayer fully detached from the cell culture insert. The absence of continuous fluid renovation was pointed out as the most probable cause for this result, as a steady circulating flow works as a way of controlling bacterial overgrowth and subsequent loss of epithelial viability. In contrast, the fluid flow established in the microfluidic device promoted the clearance of LGC metabolites and unbound microbial cells, restricting the expansion of the bacterial culture. Therefore, this gut-on-a-chip model enabled the co-culture of a commensal microorganism for more than 1 week without hampering the integrity of the epithelium.

Later in 2016, and using the system described previously (Kim et al., 2012; Kim & Ingber, 2013), Kim et al. proposed the development of a microengineered model of human inflammation and small intestinal bacterial overgrowth (SIBO) (Kim et al.,

2016). They also analysed how commensal bacteria could aid repairing the gut epithelium following inflammation-associated damage. Two strains of *Escherichia coli* (E. coli), pathogenic and non-pathogenic, were seeded over the epithelial-like tissue of the chip. As expected, pathogenic *E. coli* led to the disruption of the 3D architecture and complete loss of barrier integrity. However, this damage was diminished with the addition of commensal microbes and, later on, treatment with conventional antibiotics, such as penicillin and streptomycin. Hence, this gut-on-a-chip device could simulate protective anti-inflammatory and antibiotic treatments *in vitro*.

The authors performed an additional experiment to emulate chronic intestinal inflammation where immune cell recruitment should increase. Human peripheral blood mononuclear cells (PBMCs) were added to the endothelial-like chamber. PBMCs alone did not elicit any damage. However, when in combination with bacterial lipopolysaccharide (LPS), they enhanced the production of pro-inflammatory cytokines with subsequent severe intestinal injuries, including impairment of the barrier integrity. These results show that besides allowing the analysis of host-microbiome interactions, this microfluidic system could be used as a model of intestinal inflammation, unravelling the etiopathology of gut disorders, as well as possible therapies.

Jalili-Firoozinzehad et al. (Jalili-Firoozinezhad et al., 2019) developed a microfluidic intestine-on-chip aiming to incorporate different populations of aerobic and anaerobic bacteria originating from the human intestine. Their work succeeded by creating hypoxia gradients throughout the interfacial membrane of the chip, where both anaerobic and aerobic commensal bacteria survived for at least 5 days, in direct contact with human epithelial and endothelial cells. Moreover, they validated previous assumptions that it is possible to maintain a wider variety of microorganisms when the provided microenvironment presents appropriate levels of oxygen.

Beaurivage et al. (Beaurivage et al., 2020) set out to construct a primary gut-on-a-chip with the intent of modelling disorders such as IBD. Their device was composed of human primary intestinal epithelial cells (IEC) cultured as HIOs and integrated into the OrganoPlate® platform, along with monocyte-derived macrophages, originated from different patients. To simulate an IBD state, the device was exposed to lipopolysaccharide (LPS) and interferon-gamma (IFN-γ), which triggered the activation of proinflammatory M1 macrophages and secretion of important cytokines, resembling a natural response of the epithelium. In another study, Workman et al. (Workman et al., 2018) cultured epithelial cells obtained from iPSC-derived HIOs in microfluidic

chips and analysed their behaviour regarding multi-lineage differentiation and responsiveness towards external stimuli. The presence of the 4 main epithelial cell subtypes was confirmed by the expression of specific differentiation markers. Moreover, the cells were exposed to IFN-γ to simulate intestinal inflammation, as this cytokine is frequently augmented in gut disorders such as IBD. The results showed a similar outcome to what occurs *in vivo*, indicating that this model could be used to study biologically relevant responses of the human intestinal epithelium.

Chapter III

Materials and Methods

1. Materials and Reagents

Dow Corning Sylgard ® 184 polydimethylsiloxane (PDMS) was purchased from Ellsworth Adhesives Ibérica (Madrid, Spain). Phosphate buffered saline (PBS), ethanol, acetone, dimethyl sulfoxide (DMSO), paraformaldehyde (PFA), fluoroshield™, sodium pyruvate solution 100 mM, resazurin sodium salt, Dulbecco's modified Eagle Medium-high glucose (DMEM), disodium hydrogen phosphate (Na_2HPO_4), potassium dihydrogen phosphate (KH_2PO_4), sodium chloride (NaCl), potassium chloride (KCl), trichloro(1H,1H,2H,2H-perfluorooctyl)silane [trichlorosilane], Verapamil hydrochloride (50 mM), Rhodamine123 (100 mM), Matrigel Corning®, GF-reduced, A 83-01 (500 µM), n-Acetyl-L-cysteine (1M), [Leu15]-Gastrin I human (100 µM) and nicotinamide (1 M) were obtained from Sigma-Aldrich (St. Louis, MO, USA). 4', 6-diamidino-2-phenylindole, dilactate (DAPI, Invitrogen™), Matrigel™ membrane matrix, rat tail type-I collagen, Sulfo-SANPAH (sulfosuccinimidyl 6-(4'-azido-2'-nitrophenylamino)hexanoate), GlutaMAX Supplement, 4-(2-hydroxyethyl)-1-piperazineethanesulfonic acid (HEPES), dithiothreitol (DTT), sucrose, d-sorbitol, Advanced DMEM/F12, TrypLE™ Express Enzyme, Alexa Fluor™ 488-conjugated Occludin Monoclonal Antibody, Normal Goat Serum (NGS), Goat anti-Mouse IgG1- Alexa Fluor® 647, P-Glycoprotein Monoclonal Antibody (F4), B-27 supplement (50X) and EGF (50 $\mu g.mL^{-1}$) were obtained from Thermo Fisher Scientific (Waltham, MA, USA). Caco-2 HTB-37™ cells were purchased from the American Type Culture Collection (ATCC® HTB™). HT29-MTX-E12 cells were acquired from European Collection of Authenticated Cell culture (ECACC 12040401). Minimum essential media (MEM) Eagle was purchased from PAN-Biotech GmbH (Aidenbach, Germany). Millex-GS Syringe Filter Units 0.22, Steriflip centrifuge tube top filter unit 0.45, trypsin-EDTA (0.25% trypsin; 0.1% EDTA),

penicillin/streptomycin 100x, foetal bovine serum (FBS), Hanks' Balanced Salt Solution (HBSS) and Y-27632 Dihydrochloride (10 mM) were purchased from Merck Millipore (Burlington, MA, USA). Fungin™, Zeocin and Geneticin/G218 were obtained from InvivoGen (San Diego, CA, USA). 24-well plates were purchased from TPP Techno Plastic Products AG (Trasadingen, Switzerland). Microfluidic bubble traps were bought from Darwin Microfluidics (Paris, France). cellQART® Cell Culture Inserts were purchased from CruzLab (Vila do Conde, Portugal). Prostaglandin E2 (10 mM), SB202190 (10 mM) were obtained from MedChemExpress (NJ, USA). Supreme Sencha – Green Loose Leaf Tea was purchased from The Tea Markets of London (London, GB).

2. Microfabrication of the microfluidic device

2.1. Device design and fabrication

To fabricate flexible semi-porous membranes, silicon micropillar arrays (8-µm diameter, 32-µm pitch, 40-µm height, and offset every 2 rows - **Figure 5**) fabricated by deep reactive ion etching by the INL cleanroom team, were pre-treated with trichlorosilane (50 µL) overnight under vacuum and at 65ºC. Following silanisation, PDMS prepolymer and curing agent were mixed at a 15:1 ratio (w/w), fully degassed and poured over the silanised silicon master moulds placed on a spin coater. After a period of 5 minutes to self-spread, PDMS was spun over the silicon master moulds for 20 seconds at 500 rpm, followed by 300 seconds at 2400 rpm. After spinning, the PDMS layer was allowed to rest on the silicon master moulds for another 5 minutes, allowing the edge bead to retract. The process was completed by placing all the master moulds inside the dry oven at 65ºC for at least 1 hour and then removed to cool down to RT.

Gut-chip devices were designed using CorelDRAW from Corel Corporation (Canada). The top and bottom channels were 1 mm high by 1 mm wide and the channel geometry is shown on **Figure 5.D**).

Master moulds were manufactured on PMMA by Computer Numerical Control (CNC) machining (FlexiCAM Viper CNC, FlexiCAM GmbH, Eibelstadt, Germany). To prepare top and bottom slabs, PDMS prepolymer and curing agent were mixed at a 15:1 ratio (w/w), fully degassed and poured over the PMMA moulds. PDMS bottom slabs were bonded to the fabricated PDMS membranes on the pillar arrays by oxygen plasma. Inlets and outlets were punched into the top PDMS slab, using 1.5-mm diameter biopsy

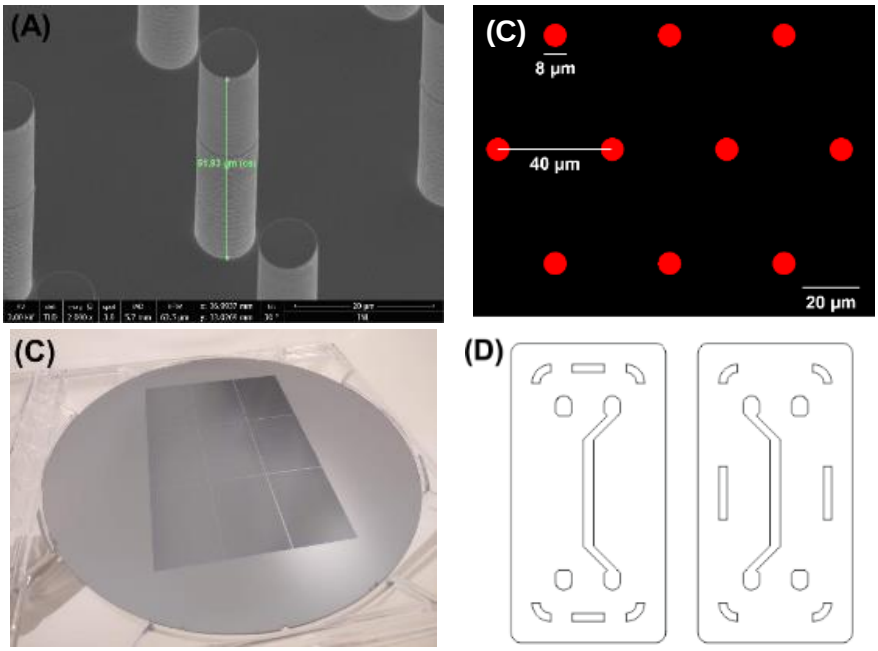

Figure 5 - (A, B) *SEM images of silicon master moulds with micropillar arrays,* ***(C)*** *silicon master moulds. Images were taken by the International Iberian Laboratory Nanotechnology (INL), Portugal, cleanroom staff.* ***(D)*** *Mask design of top and bottom slabs of the gut-chip.*

punches. The bottom and top channels were oxygen plasma treated and bonded under a magnifying lamp, using an alignment equipment engineered in-house, so that the channels of the two layers overlapped. The assembly was then placed in a dry oven at 65ºC for 15 minutes, to achieve irreversible bonding.

3. Cell culture and expansion

3.1. Cell culture

Caco-2 HTB-37™ cells (passages 40 to 52) were expanded in minimum essential media (MEM), supplemented with 20% FBS, 1% sodium pyruvate, 100 U·mL^{-1} Penicillin and 100 µg·mL^{-1} Streptomycin (1% Pen/Strep). Cells were maintained in a humidified chamber at 37ºC and a 5% CO_2 atmosphere. MEM was replenished every 2-3 days and cells were regularly sub-cultured at a maximum confluence of 70-80%. Adherent cells were detached using Trypsin-EDTA for 5 minutes.

HT29-MTX-E12 cells (passage 80), were expanded in Dulbecco's Modified Eagle Medium (DMEM), supplemented with 10% FBS and 1% Pen/Strep. Cells were maintained in a humidified chamber at 37ºC and a 5% CO_2 atmosphere. DMEM was replenished every 2-3 days and cells were regularly sub-cultured at a maximum confluence of 70-80%. Adherent cells were detached using Trypsin-EDTA for 5 minutes.

Both cell cultures were individually maintained off-chip and single cultures of Caco-2 cells on 24-well plates, as described above. For co-cultures, cells were used at a 9:1 ratio (Caco-2/HT29-MTX).

3.2. Static culture on cell culture inserts

Static cultures of Caco-2 cells in cellQART® cell culture inserts containing porous polyester membranes (0.3 cm^2, 1-µm pores) were used as control. Cells were seeded at $1x10^5$ $cells.cm^{-2}$ and the medium was routinely changed every 2-3 days. TEER was measured every 7 days.

3.3. On-chip cell culture

This procedure encompasses the following steps: device sterilisation, PDMS membrane functionalisation, cell seeding and on-chip cell culture, with continuous culture media perfusion.

Gut-chip devices were sterilised inside a laminar flow hood using 70% (v/v) ethanol and UV exposure for 30 minutes. The channels were then flushed with PBS. The PDMS membranes were functionalised by adding Sulfo-SANPAH (0.5 $\mu g \cdot mL^{-1}$) to the top channel, followed by its photo-activation by UV radiation (λ=365 nm; 6.8 W; distance: 5 cm) for 30 minutes. The solution was removed, and the device washed with sterile diH_2O, followed by cold PBS. An ECM solution of rat type I collagen (30 $\mu g \cdot mL^{-1}$) and Matrigel® (100 $\mu g.mL^{-1}$) in serum-free DMEM was introduced in the upper channel and incubated at 4ºC overnight plus 1h at 37ºC the following day. The ECM solution was removed from the upper channel and washed with serum-free media to remove excess ECM.

Caco-2 cells were introduced into the upper microchannel at a cell density of $1x10^5$ $cells.cm^{-2}$, followed by overnight incubation at 37ºC to enable cell adhesion to the ECM-coated membrane. The devices were then connected to a syringe pump system using polytetrafluoroethylene (PTFE) tubing. All the tubing and fittings were always sterilized by autoclaving. The culture medium was degassed using a Steriflip centrifuge tube top filter unit with a 0.45-µm pore size poly(vinylidene fluoride) membrane, and further degassed in a desiccator for about 30minutes. The inlets were connected to pre-filled sterile 10 mL syringes via 0.5-mm ID, 1.6-mm OD PTFE tubing and 24-gauge syringe needles primed with supplemented MEM. The syringes were placed on an in-house built pumping system to allow continuous culture media perfusion through both top and bottom channels, at a constant flow rate (120 $\mu g \cdot mL^{-1}$). PTFE tubing connected

the outlets to external reservoirs to collect the outflow culture medium. The whole setup (**Figure 6**) was placed in an incubator at 37 °C and 5% CO_2. Autoclavable microfluidic bubble traps were included to prevent air bubbles in the tubing from entering the chip channels.

4. P-glycoprotein inhibition assay

A P-glycoprotein (P-gp) inhibition assay was conducted to validate the gut-chip model for functional intestinal absorption studies. Caco-2 cells were used for expressing P-gp at levels similar to those observed in the normal human jejunum. Moreover, the Caco-2 cell line is validated for P-gp substrates screening (Martins et al., 2019; Rocha-Pereira et al., 2020; Silva et al., 2015).

P-gp is an efflux pump protein mainly expressed in epithelial tissues, such as the intestinal epithelium (Frances J. Sharom, 2011). Rhodamine 123 (Rho123) is a P-gp fluorescent substrate, which is transported across Caco-2 monolayers via transcellular and paracellular pathways (Troutman & Thakker, 2003), and is frequently used to assess P-gp efflux function through standard permeability assays (J. S. Lee et al., 1994).

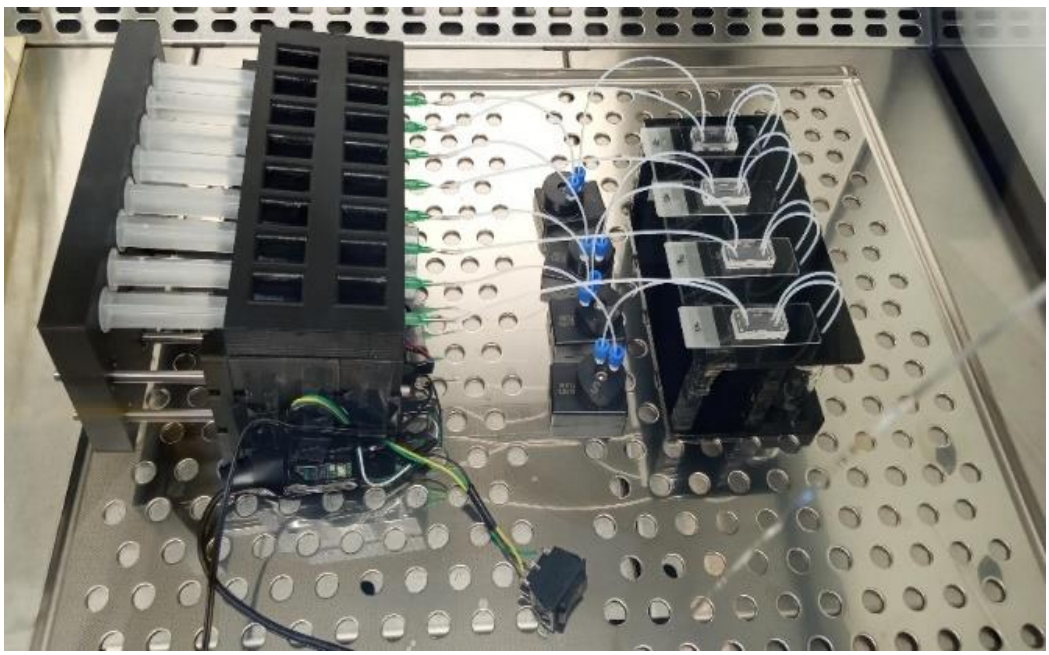

***Figure 6** - Culture media perfusion on chip.*

4.1. Permeability Assay

Green tea (GT) was prepared by brewing 2.5g of commercial GT leaves in 100 mL of water at 85ºC for 5 minutes. The leaves were then separated using a tea strainer and the tea diluted in HBSS (1:10). GT was used a natural P-gp inhibitor. Rho123 was used at 50 µM diluted in HBSS as a P-gp efflux reporter, and verapamil (VRP) was used at 25 µM in HBSS as a positive control of P-gp inhibition. The apparent permeability coefficient (P_{app}) of Rho123 was calculated according to Equation 1.

$$P_{aap} = \left(\frac{dC/dt \times V}{C_0 \times A} \right) [cm.s^{-1}] \qquad \textit{Equation 1}$$

Where ***dC/dt*** is the permeation rate ($\mu M.s^{-1}$) of the Rho123 across the cells, i.e., the change in concentration per time unit; C_0 is the concentration of Rho123 (50 µM) at time zero, ***A*** is the area (cm^2) of the cell monolayer and ***V*** is the volume (cm^3) of the donor chamber.

4.1.2. Bidirectional transport studies in Caco-2 monolayer model

Caco-2 cells were seeded on the apical chamber of cell culture inserts at a cell density of $1x10^5$ cells.cm^{-2}. The culture was maintained for 21 days, as the standard period of time leading to full cell differentiation in static conditions. On day 21, the culture media was removed, and cells were washed twice with pre-warmed HBSS. The inserts were then transferred to a new 24-well plate, pre-filled with warm HBSS, and the plate was placed in an orbital shaker for 30 min, at 37ºC and 100 rpm, to allow cells to equilibrate.

The TEER was then measured in each well to assess the monolayer integrity. HBSS was removed from each donor chamber, and test solutions (Rho123 in isolation, Rho123+VRP or Rho123+GT) were added to the donor chambers (apical or basolateral) accordingly. Where VRP and GT were used, these were also added to the receptor chambers but in the absence of Rho123. The transport of Rho123 across the monolayer was monitored over a 4-hour period by taking 100-µL aliquots from the receiving chambers every hour. The volume collected was replenished with 100 µL of HBSS to maintain sink conditions. At each time-point, the fluorescence of Rhodamine 123 were measured using a microtiter plate reader (Synergy H1, Biotek Microtiter Plate Reader, controller software: Gen5), with excitation/emission wavelengths of 467/529 nm.

The efflux ratio (ER) is defined as the ratio of flux from the basolateral to the apical compartment over that from apical to basolateral compartment and was calculated according to Equation 2.

$$\text{Efflux Ratio} = \frac{P_{app}^{BA}}{P_{app}^{AB}} \qquad \textit{Equation 2}$$

Where $\mathbf{P_{app}^{AB}}$ and $\mathbf{P_{app}^{BA}}$ correspond to the apparent permeability coefficients ($cm.s^{-1}$) from the apical to the basolateral side, and from the basolateral to the apical side, respectively.

4.1.2.1. TEER measurements

To evaluate the cell monolayer integrity throughout the assay, the TEER (Transepithelial Electrical Resistance) was measured using Millicell® ERS-2 Voltohmmeter and STX chopstick electrodes. The TEER ($\Omega \bullet cm^2$) was calculated by subtracting the readings of cell-free inserts from the cell cultured inserts and multiplying by the surface area of the membrane (0.3 cm^2).

4.1.3. Assay on a microfluidic device

To replicate the P-gp inhibition assay on-chip, 50 µM Rho123 in HBSS with or without 25 µM VRP were perfused through the bottom channels of gut-chip devices, at a constant flow rate of 20 $\mu L.h^{-1}$. The top channels were perfused with HBSS solutions with or without 25 µM VRP correspondingly. 20-µL samples were collected from both inlets and outlets at 4 different time points: 2, 3, 4 and 5 hours. **Figure 7** shows the experimental setup used in this assay.

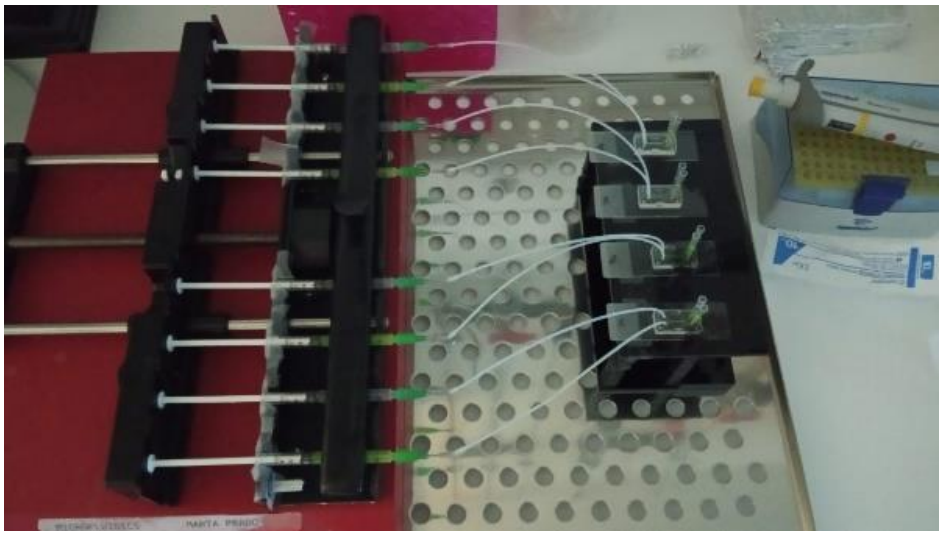

***Figure 7** – Assay on chip setup.*

4.2. Immunocytochemistry

At the end of each experiment, cells were fixed with 4% (w/v) paraformaldehyde (PFA) for 15 minutes and permeabilised by incubation at 4ºC with a 0.2% (v/v) Triton X-100 solution in PBS, for 10 minutes. The fixed cells were incubated with a 5% (w/v) NGS solution in PBS (blocking buffer) for 60 minutes at RT to minimise non-specific antibody bonding. After blocking, cells were incubated with a solution of 0.2 $\mu g \cdot mL^{-1}$ P-gp Monoclonal Antibody and 5 $\mu g \cdot mL^{-1}$ Alexa Fluor® 488-conjugated occludin monoclonal antibody (OC-3F10) overnight, at 4ºC. After extensive washing, cells were stained with 1 $\mu g \cdot mL^{-1}$ Goat anti-Mouse IgG1-Alexa Fluor® 647 for two hours at RT and counterstained with 1 $\mu g \cdot mL^{-1}$ DAPI for 10 minutes.

Alexa Fluor® 488 conjugated with OC-3F10 was used to stain Occludin, a tigh junction protein. Alexa Fluor® 488 maximum excitation (λ_{ex}) and emission (λ_{em}) wavelengths are at 499 and 520 nm, respectively. Cell nuclei were stained using DAPI $\lambda ex/\lambda em$ = 360/463 nm. Alexa Fluor® 647 enabled P-gp observation at $\lambda ex/\lambda em$ = 649/670 nm.

Caco-2/HT29-MTX co-cultures were fixed using a similar procedure, but thereafter incubated with a 2% (w/v) BSA solution in PBS (blocking solution/buffer) for 30 minutes to minimise non-specific antibody bonding. After blocking, cells were incubated with 5 $\mu g \cdot mL^{-1}$ Alexa Fluor® 488, conjugated occludin monoclonal antibody (OC-3F10) and 0.1 $\mu g \cdot mL^{-1}$ phalloidin-TRITC overnight, at 4ºC. After extensive washing, cells were counterstained with 1 $\mu g \cdot mL^{-1}$ DAPI for 10 minutes and preserved in fluoroshield mounting media.

4.3. Laser Scanning Confocal Microscopy (LSCM)

Cell culture membranes were cut using a scalpel and mounted on a glass slide with a drop of fluoroshield mounting media. The membranes were covered with a coverslip and sealed with nail polish. Images of gut-chips and cell culture inserts were taken using a confocal microscope (LSM 780, Zeiss) equipped with 405-nm and 561-nm diode lasers and a 488-nm argon laser. Images were taken at 10x, 20x, 40x and 63x magnification in oil and analysed using Zen 2010 software and ImageJ.

4.3. Statistical Analysis

All data is presented as mean ± standard deviation (SD) of six independent experiments. Significant differences in the P_{app} and efflux ratio values were evaluated by performing a repeated measure 2-way ANOVA followed by Dunnett's multiple comparisons test, for cell culture inserts. For the assays on gut-chip devices, significant differences in the P_{app} values were analysed by performing a repeated measure 1-way ANOVA, followed by Welch's t test. All analyses were done using GraphPad Prism 9.2.0 (GraphPad Software Inc., San Diego, CA, USA).

5. Primary cell isolation and expansion

5.1. Primary intestinal cells isolation and cryopreservation

5.1.2. Media and buffer preparations

Collection Medium

Collection medium (CM) consisted of Advanced DMEM supplemented with GlutaMAX (1X), HEPES (10 mM), 1% Pen/Strep and 1 mg·mL^{-1} Fungin™.

Colon crypt Isolation Buffer

For the preparation of the Isolation/Washing buffer (WB), Na_2HPO_4 (5.6 mmol.L-1), KH_2PO_4 (8.9 mmol.L-1), NaCl (96.2 mmol.L-1), KCl (1.6 mmol.L-1), sucrose (43.4 mmol.L-1), and d-sorbitol (54.9 mmol.L-1) were solubilized in diH_2O, filter sterilised and stored at RT until further use.

Dissociation Buffer

Dissociation buffer (DB) was freshly prepared every time by adding 2 mM EDTA and 0.5 Mm DTT to the WB.

Conditioned Medium

L-wnt3a and HEK-293-mNoggin-Fc cells were kindly offered by Hans Clever's laboratory (Hubrecht Institute, KNAW and University Medical Centre Utrecht, Utrecht, The Netherlands). The conditioned media was obtained following a protocol similar to the one reported in (Sato et al., 2009, 2011) with some adjustments, as follows.

- Noggin conditioned media

HEK-293-Noggin cells were expanded in DMEM, supplemented with 10% FBS, 1% Pen/Strep and 100 mg.mL^{-1} Geneticin (selection media). Cells were maintained in a humidified chamber at 37ºC and 5% CO_2 atmosphere. DMEM was replenished every

other day until reaching confluence of 70-80%. The growth media was replaced by conditioning media, composed of Advanced DMEM, supplemented with 1% HEPES (1 M), GlutaMAX (1X) and 1% P/S. After one week, the supernatant was harvested by centrifugation for 5 minutes at 450 g, sterile filtered through a 0.22 µm Polyethersulfone (PES) membrane and stored at -20ºC/-80ºC for future use.

- Wnt-3a conditioned media

L-wnt3a cells were expanded in DMEM, supplemented with 10% FBS, 1% Pen/Strep and 100 $mg.mL^{-1}$ Zeocin (selection media). Cells were maintained in a humidified chamber at 37ºC and 5% CO_2 atmosphere. DMEM was replenished every other day until reaching confluence of 70-80%. Zeocin was then removed from the media and after one week, the supernatant was harvested by centrifugation for 5 minutes at 450 g, to remove floating cells, sterile filtered through a 0.22 µm PES membrane and stored at -20ºC/-80ºC until further use.

Expansion Media (EM)

Expansion Media was prepared fresh by combining both collection and conditioned media with multiple other factors, as described in (Ordóñez-Morán, 2020). The final volumes and concentrations of each reagent for a volume of 100 mL are presented in **Table 1**.

***Table 1** - Primary cell culture media formulation.*

Component	Stock concentration	Volume required for 100 mL	Final concentration
Collection Media	-	22 mL	-
Wnt-conditioned media	-	50 mL	50%
R-Spondin1-conditioned media	-	20 mL	20%
Noggin-conditioned media	-	5 mL	5%
A 83-01	500 µM	100 µL	500 nM
n-Acetyl-L-cysteine	1 mM	100 µL	1 mM
B-27 Supplement minus Vit.A	50X	2 mL	1X
EGF	50 µg/mL	100 µL	50 ng/mL
[Leu15]-Gastrin I human	100 µM	10 µL	10 nM
Nicotinamide	1 M	1 mL	10 mM
Prostaglandin E2	10 mM	10 µL	1 µM
SB202190	10 mM	100 µL	10 µM
Y-27632 Dihydrochloride	10 mM	10 µL	10 µM

5.1.3. Intestinal crypt isolation and cryopreservation

Intestinal tissue samples (small intestine and colon) were collected from human patients undergoing small intestine or colonic surgeries, as part of their ongoing medical treatment at Hospital de Braga (Braga, Portugal) and with full patient consent

and approval by an Ethics committee (ref. 62_2021. The samples were transported to the laboratory in 50-mL centrifuge tubes previously filled with 25 mL CM, in a sealed ice box. Samples were preferably processed straight away or within the next 24 hours, in which case they were stored at 4ºC.

CM was discarded and the tissue sample transferred to a Petri dish, following extensive washing with WB at RT. Fat was removed using scalpels and tweezers. The sample was then transferred to a new 50-mL tube pre-filled with 25 mL of WB for further washing and finally transferred to another 50-mL tube containing 25 mL of DB, and incubated for 1 hour at RT. After incubation, the tube was vigorously shaken by hand and the supernatant was checked for the presence of crypts. This step was repeated 3 to 4 times with 30 minutes' incubation steps. Finally, the tubes were centrifuged at 180 g, for 5 minutes at 4ºC or at RT, the supernatant discarded, and the pellet carefully re-suspended in 10 mL CM. Isolated crypts were counted under an optical microscope from a 10-µL drop and cryopreserved at 500 crypts/mL.

5.2. Organoid culture

Isolated crypts were resuspended in Matrigel® at 10 crypts/µL seeding density. The whole procedure was done on ice and using cold pipette tips to prevent Matrigel gelification. 20 to 25-µL drops of crypt suspension in Matrigel were seeded at the bottom of the wells of a pre-warmed 6-well plate. The plate was then incubated inverted at 37ºC for 20-30 minutes to allow dome formation and crypts to spread throughout. Thereafter, EM (10 µM), supplemented with Y-26732, was added to each well. Organoid cultures were maintained in a humidified chamber at 37ºC and a 5% CO_2 atmosphere. EM was changed every two days, without Y-26732 supplement and the organoids were passaged every one or two weeks.

Chapter V

Results and Discussion

1. Establishment of a Gut-Chip platform

1.1. Device fabrication

Device fabrication steps are represented in **Figure 8**.

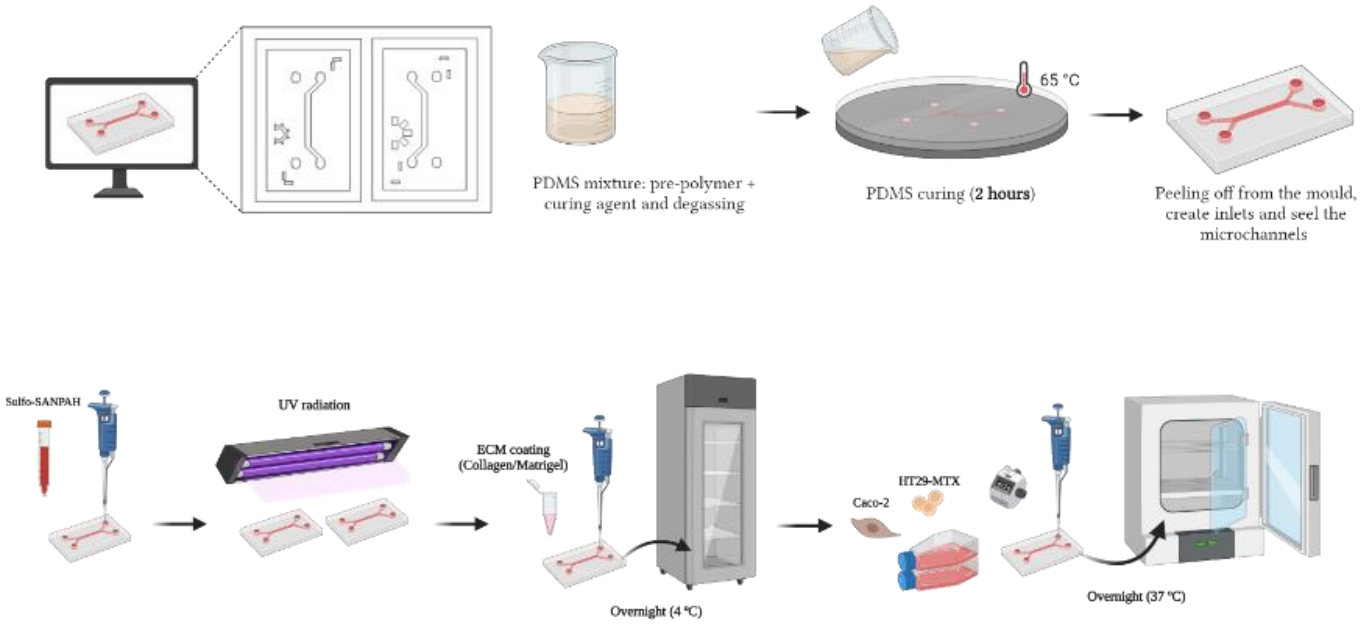

***Figure 8** - Schematics of the main steps of the PDMS device fabrication and subsequent functionalisation and ECM coating of the porous membrane. Image created with Bioreder.com by Patrícia M. Rodrigues from the Food Processing and Nutrition Group (FPNG), INL.*

1.2. On-chip cell culture

Caco-2/HT29-MTX (9:1) co-cultures were established on cell culture inserts and in the gut-chip under static conditions or continuous flow respectively. Cell morphology and polarization, and the establishment of an epithelial barrier, were assessed by immunocytochemistry using an antibody against the tight junction protein occludin, rhodamine-labelled phalloidin to stain F-actin and DAPI to stain nuclei.

Continuous flow appeared to influence cell polarisation with the presence of basal nuclei (columnar shape) as can be seen in **Figure 9**. Therefore, application of flow in the apical cell surface promoted faster cell differentiation which was noticed by polarisation of these cells under fluid flow at day 7. Moreover, cells grown on-chip formed an epithelium with a 3D architecture similar to intestinal villi. In contrast, cells grown in culture inserts systems remained flat even after 3 weeks, as can be confirmed by the orthogonal images in **Figure 10**.

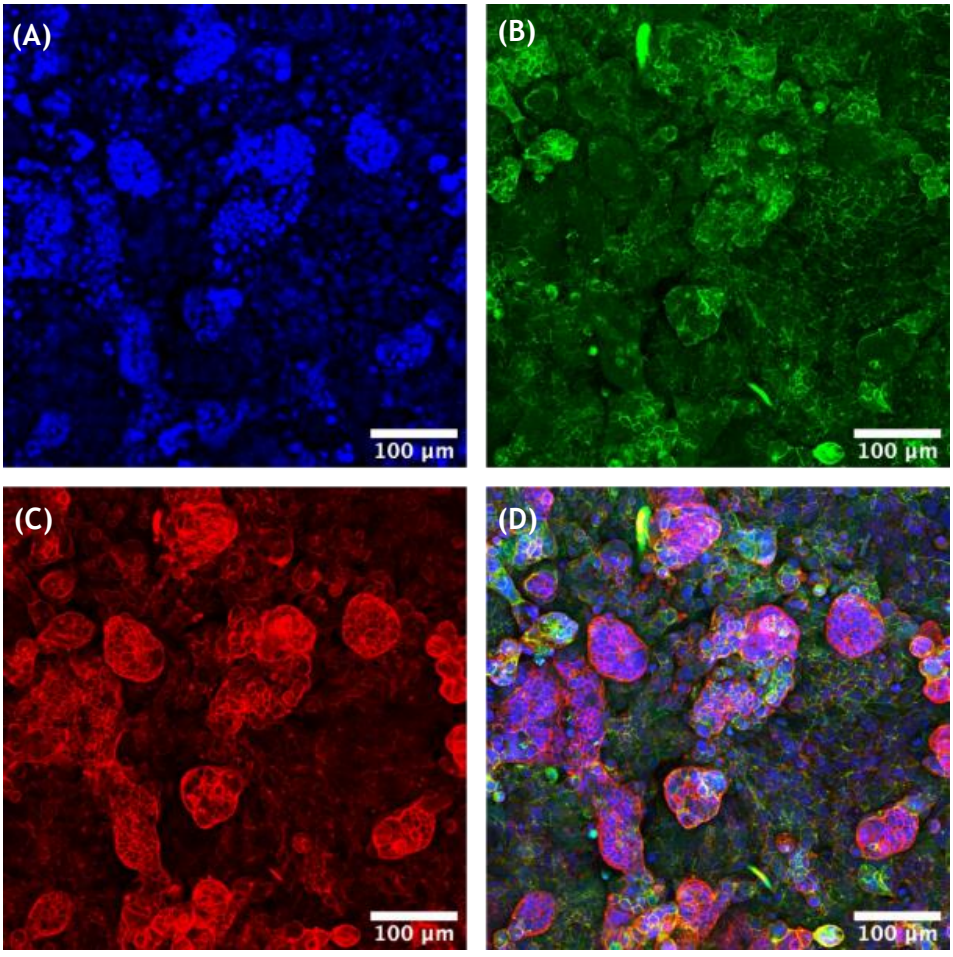

Figure 9 *- Z-projected confocal microscopy images of Caco-2/HT29-MTX co-culture on-chip under continuous flow (120 µL.h^{-1}) for 7 days, 40× magnification. (A) Nuclei stained with DAPI; (B) Occludin stained with AF488-Anti-Occludin; (C) F-actin stained with Phalloidin-TRITC; (D) Merged signals. Images were collected by an MSc student from the FPNG - M.I.Guedes.*

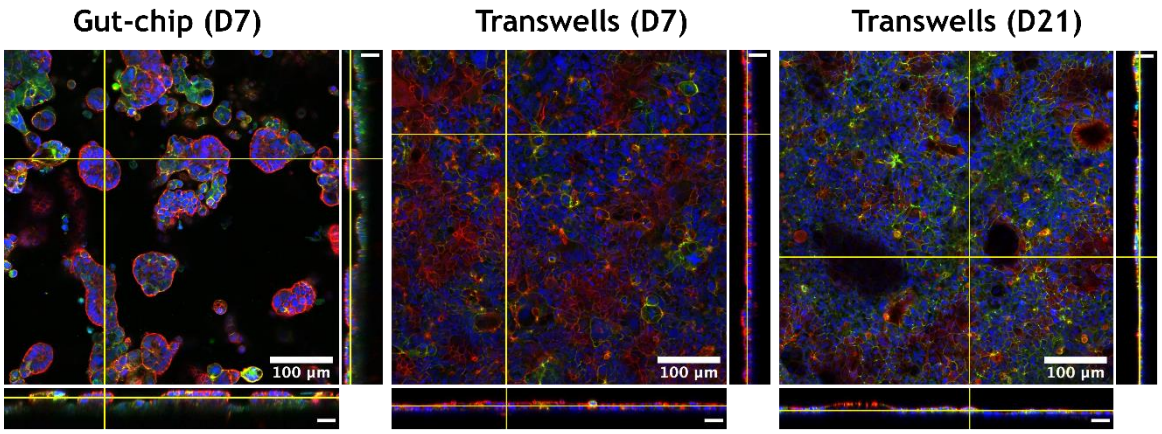

Figure 10 - *Confocal images and orthogonal cross-section views of Caco-2/HT29-MTX co-cultures on gut-chip after 7 days of continuous flow (120 µL·h^{-1}) (left pannel) and Transwell inserts after 7 days (middle panel) and 21 days (right pannel) in culture, stained for occludin (green), nuclei (DAPI, blue) and F-actin (red). Bar in the orthogonal images corresponds to 30 µm. Images were collected by M.I.Guedes*

These results are in line with other experiments regarding cell culture on gut-chip systems (Kim & Ingber, 2013; Shim et al., 2017), where the authors describe that fluid perfusion promoted cell differentiation and villi formation.

Figure 11 shows equivalent confocal microscopy images of Caco-2 cells grown on-chip under continuous media perfusion and on cell culture inserts after 7 (D7 on-chip) and 21 (D21 inserts) days of culture respectively. Although nuclei number is significantly different, occludin expression was observed in both models.

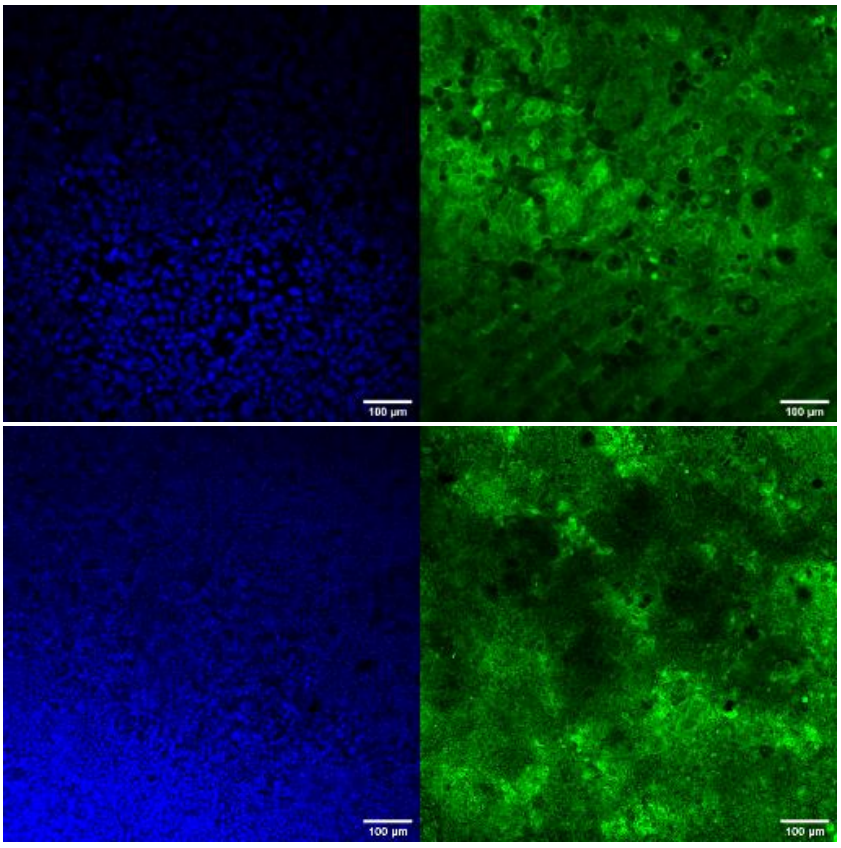

Figure 11 *– Confocal laser scanning microscopy images of Caco-2 cultured (top pannel) on-chip for 7 days under continuous flow (120 µL.$^{-1}$) and (bottom pannel) on cell culture inserts, under static conditions, for 21 days. Both cell cultures were stained for nuclei (blue), occludin (green), 10× magnification.*

2. Functional on-chip assay targeting the inhibition of an efflux transporter (P-gp)

P-glycoprotein (P-gp) is an efflux transporter with broad substrate specificity, including fluorescent dyes such as Rhodamine 123 (Rho123). In this work, Rho123 transport across two *in vitro* models of epithelial intestinal tissue was quantified to assess P-gp activity in the presence of two inhibitor molecules.

P-gp is predominantly located on the apical surface of the intestinal epithelium. Thus, when observing apical to basolateral (AB) transport, reduced amounts of P-gp substrates are expected on the basolateral chamber, as these will be effluxed back to the apical side through active transport. Only a smaller amount would be crossing the cellular epithelium via diffusion and start accumulating on the basolateral side. On the opposite direction however, a higher increase in concentration is expected due to continuous efflux by P-gp.

2.2. Static culture

For the bidirectional transport experiments, a 50 μM Rho123 solution, alone or in the presence of verapamil (VRP) or green tea (GT), was added to the donor chamber. The apparent permeability coefficient (P_{app}) and the efflux ratio (ER) of Rho123 were determined in each experimental group to investigate the effects of VRP and GT on P-gp efflux activity (**Figure 12**).

The data in **Figure 12** shows a clear distinction between AB and BA transports. Regarding AB transport, there was a slight decrease in the P_{app} of Rhodamine 123 in the presence of VRP and GT, but with no significant differences when compared to the Control. For BA transport, there was a significant decrease ($p < 0.0001$) in P_{app} values in the presence of VRP and GT. The evident difference between AB and BA transports indicates that Rho123 transport does not occur only via diffusion across the cell monolayer. P-gp is pumping Rho123 out of the cells, by active transport, as stated in previous studies (Troutman & Thakker, 2003).

ER values (**Figure 12.B**) decreased from Control to Verapamil: 9.838 ± 5.530 (Control), 6.116 ± 1.421 (GT) and 4.460 ± 1.739 (VRP), which indicates that Green Tea can function as a P-gp inhibitor as well.

VRP inhibited BA transport of Rho123, which is consistent with the fact that this molecule is a well-known P-gp inhibitor (G. Lee et al., 2018). Despite the proven

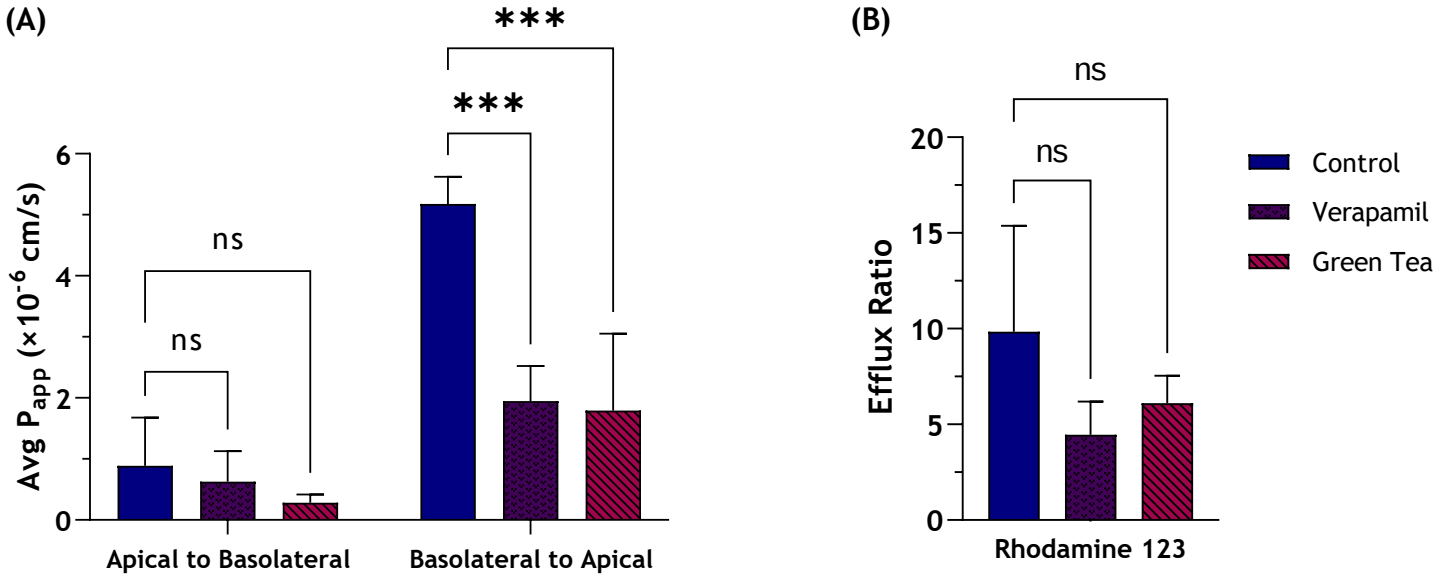

Figure 12 *- Apparent permeability coefficient (A) and efflux ratio (B) of Rhodamine 123 on Caco-2 grown on cell culture inserts. Bidirectional transport of Rho123 was assessed for 3 experimental conditions after 21 days of culture. The values are presented as means ± SD (n=3; statistical significance p < 0.0001)*

efficacy of Verapamil and other synthetic inhibitors, these are associated with high toxicity (Abdallah et al., 2015).Thus, inhibitors of natural origin arise as alternatives (Abdallah et al., 2015), as is the case of GT. GT exerted similar effects to VRP in this study. These results are consistent with previous statements of GT activity as a P-gp inhibitor (Zhang et al., 2004, 2006).

In addition, TEER values did not change (**Figure 13**) and P-gp expression was similar among all 3 conditions (**Figure 14 - Figure 17**). This supports the hypothesis that the differences in Rho123 P_{aap} values were due to P-gp inhibition and not to a compromised epithelial monolayer or reduced P-gp expression.

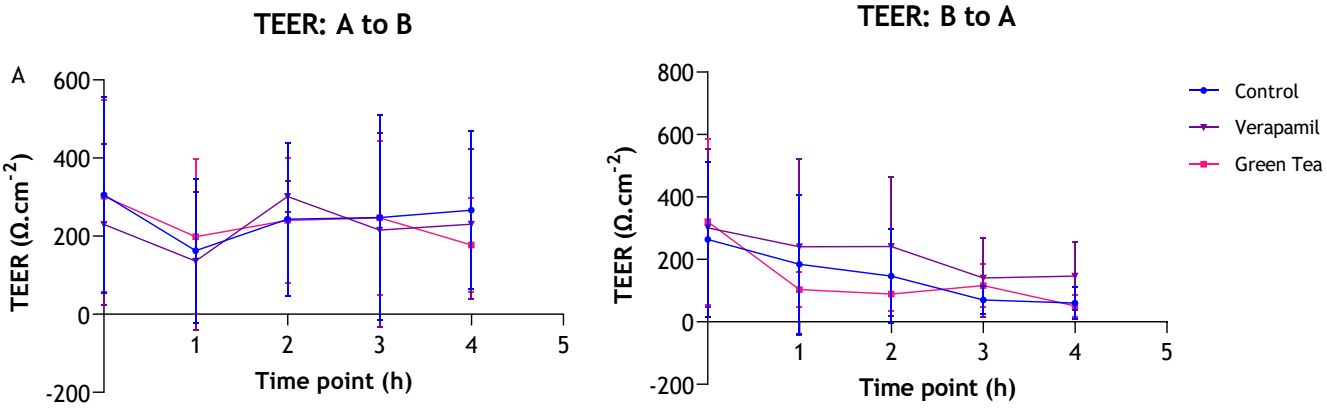

Figure 13 *- TEER values: A to B - Apical to Basolateral side; B to A - Basolateral to Apical side.*

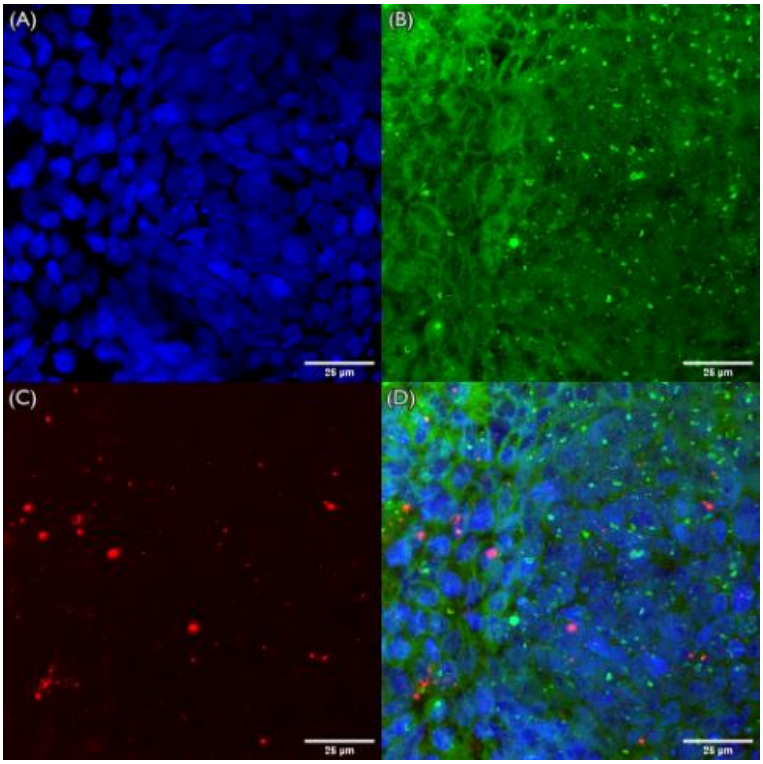

Figure 14 *- Control. Z-stacked confocal microscopy image of Caco-2 cultured on cell culture inserts for 21 days, under static conditions, 63× magnification. (A) Nuclei stained with DAPI; (B) Occludin stained with AF488-Anti-Occludin; (C) P-glycoprotein stained with AF647; (D) Merged signals.*

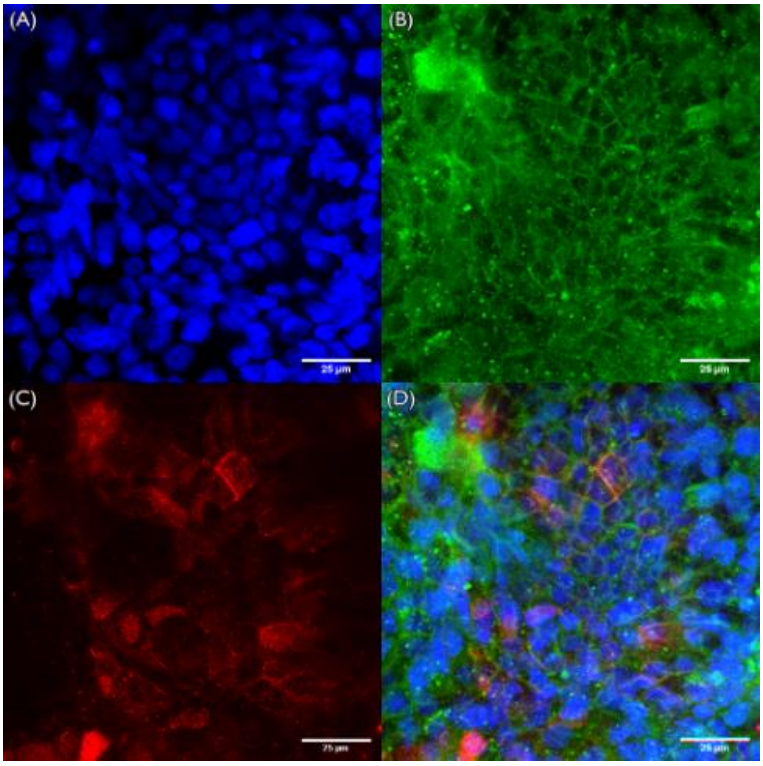

Figure 15 *- Verapamil influence on P-gp expression. Z-stacked confocal microscopy image of Caco-2 cultured on cell culture inserts for 21 days. under static conditions, 63× magnification. (A) Nuclei stained with DAPI; (B) Occludin stained with AF488-Anti-Occludin; (C) P-glycoprotein stained with AF647; (D) Merged signals.*

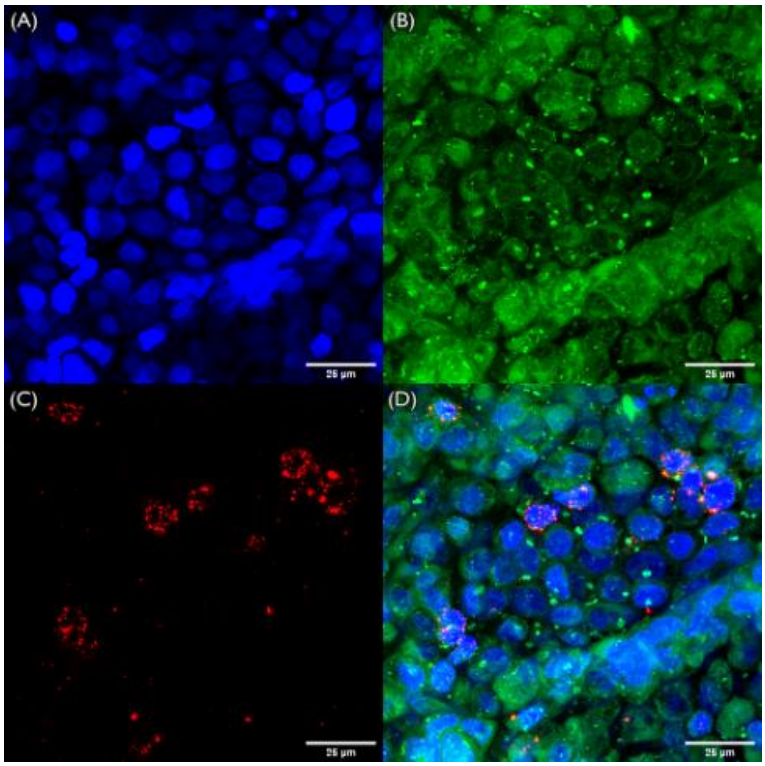

Figure 17 *– Green Tea influence on P-gp expression. Z-stacked confocal microscopy image of Caco-2 cultured on cell culture inserts for 21 days. under static conditions (63× magnification). (A) Nuclei stained with DAPI; (B) Occludin stained with AF488-Anti-Occludin; (C) P-glycoprotein stained with AF647; (D) Merged signals.*

2.2. On-chip culture

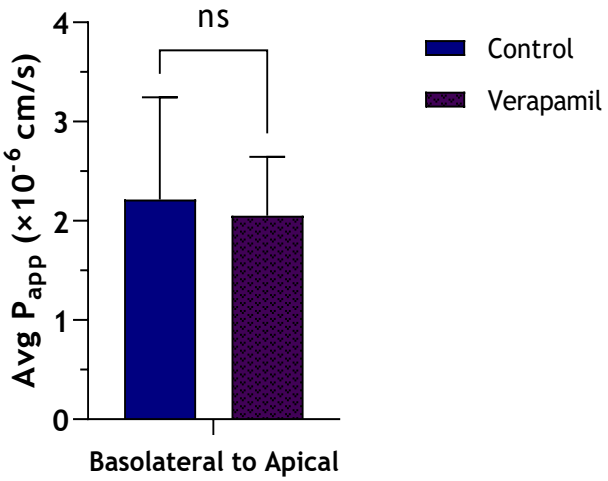

Figure 16 - *Apparent permeability coefficient of Rhodamine 123 on Caco-2 grown on-chip. Rho123 uptake was assessed in the presence or absence of Verapamil, after 7 days of culture. The values are presented as means ± SD (n=3; statistical significance p < 0.05).*

Inhibition of P-gp activity on-chip returned P_{app} values of Rho123 that were equivalent to the static cultures (**Figure 16**), which validates the use of the gut-chip for permeability assays. However, Rho123 transport in the control was equally reduced indicating in no significant differences between the 2 conditions, in contrast to what was observed in the cell culture inserts. This may be justified by difficulties in sampling from the gut-chip that frequently resulted in backflow from outlets and may compromise results interpretation. The development of an automated sampling mechanism is part of the group's current research goals. **Figure 18** was retrieved from the dynamic culture on-chip, in the presence of Verapamil. As expected, P-gp is predominantly observed in the apical regions of the cells and the presence of inhibitors did not seem to impact P-gp expression on the cells.

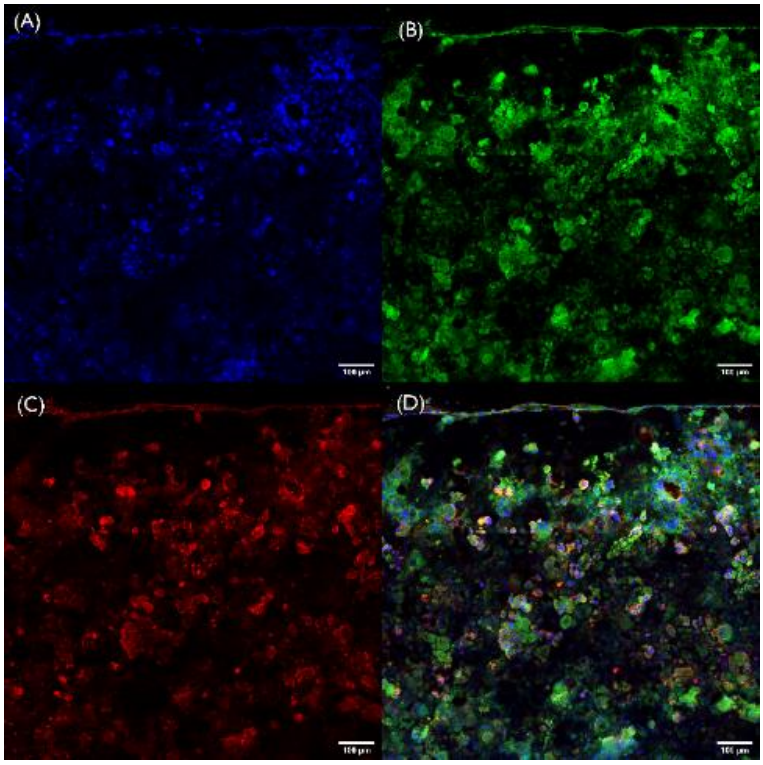

Figure 18 *- Verapamil influence on P-gp expression. Z-stacked confocal microscopy image of Caco-2 cultured on-chip, under continuous flow for 7 days, 40× magnification. (A) Nuclei stained with DAPI; (B) Occludin stained with AF488-Anti-Occludin; (C) P-glycoprotein stained with AF647; (D) Merged signals.*

3. Primary cell isolation and organoid culture

3.1. Intestinal crypts isolation

Intestinal crypts were isolated from distinct regions of the intestine (small intestine and colon) of primary tissue samples collected from patients undergoing tumour resection surgeries at Hospital de Braga. The samples were processed at different time points after collection and with variations in temperature during the incubation steps.

Figure 19 shows that when isolation was conducted at room temperature (**Figure 19.A-C**), crypts structure tended to exhibit more fragmentation than when isolation was at 4ºC (**Figure 19.D-F**). In addition, crypts isolated from the ileum (small intestine - **Figure 20.C-D**) appear to be retrieved at higher numbers than the ones from the colon (**Figure 20.A-B**).

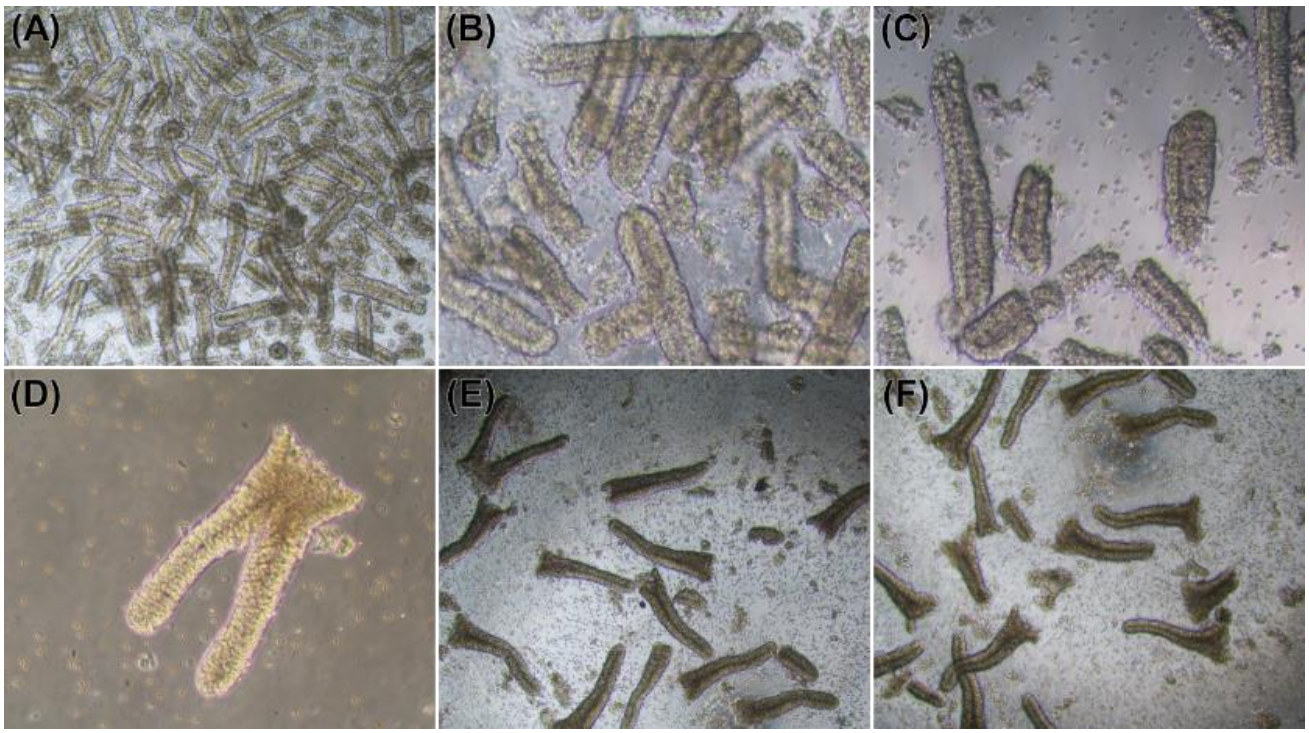

***Figure 19** - Optical microscopy images of intestinal crypts isolated at different temperatures: (top panel) room temperature, (bottom panel) 4ºC; (A, D) before and (B-C, E-F) after centrifugation. [(A, E, F) 4x magnification, (D, B, C) 10x magnification].*

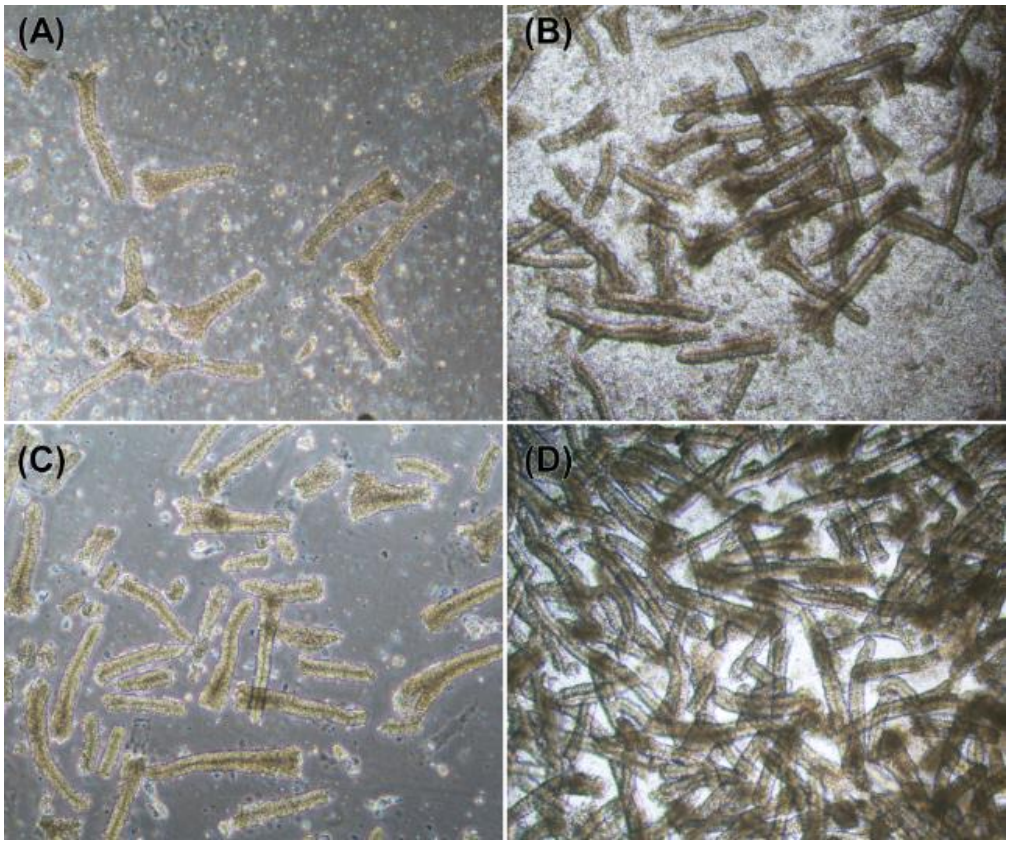

***Figure 20** - Optical microscopy images of colon crypts (A, B) and ileum crypts (C, D) before (left panel) and after (right panel) centrifugation, 4x magnification*

Although not shown here, it was also possible to note that tissue samples processed within less than 24 hours after collection would allow the isolation of more structured intestinal crypts, whereas after that time crypts would turn up more fragmented. These alterations may reflect the loss of other supporting cells in time (Fuller et al., 2012). This impacted organoid formation, which was only successful using intestinal crypts obtained from fresh intestinal samples (up to 24h post-surgery).

3.2. Organoid culture

Crypt isolation was followed by organoid culture. It was possible to observe the formation of organoid-like structures, even though the majority could not be maintained for more than 4-5 days after culture (**Figure 21**) since the spheric architecture would be lost (**Figure 22.D**).

Figure 21 shows a representative image of an organoid culture maintained for 4 days. The structures start to grow from the crypts exhibiting an ellipsoid-like appearance (A). Later, they start to detach (B) and acquire a more spherical aspect (C). Although some cultures could reach day 7 without completely losing their spherical

shape, it was not possible to successfully subculture them as all the structure was lost in the process (**Figure 22**).

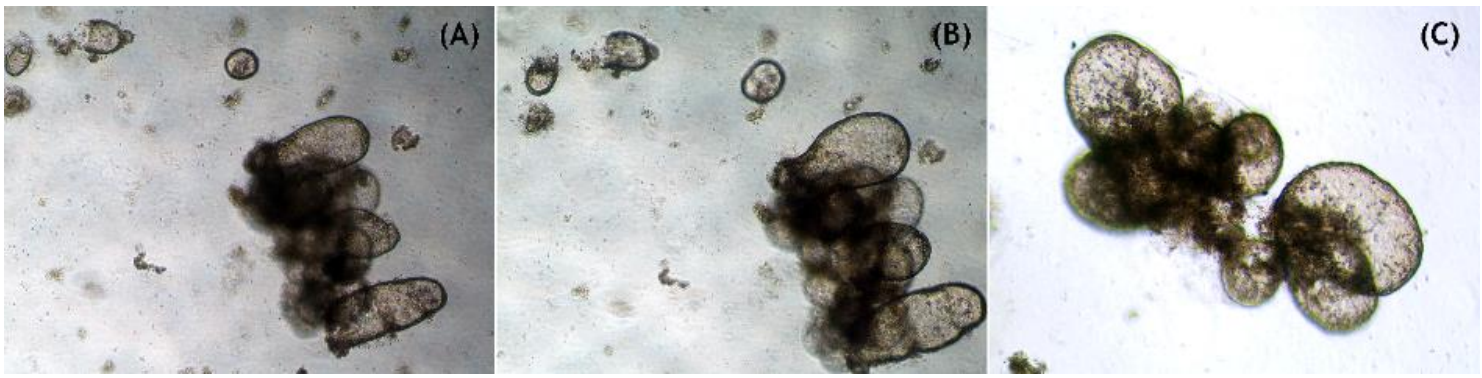

***Figure 21** - Optical microscopy images of organoid-like structures derived from colon crypts. (A) Day 1 (B) day 2 (C) day 4 after culture, 4x magnification.*

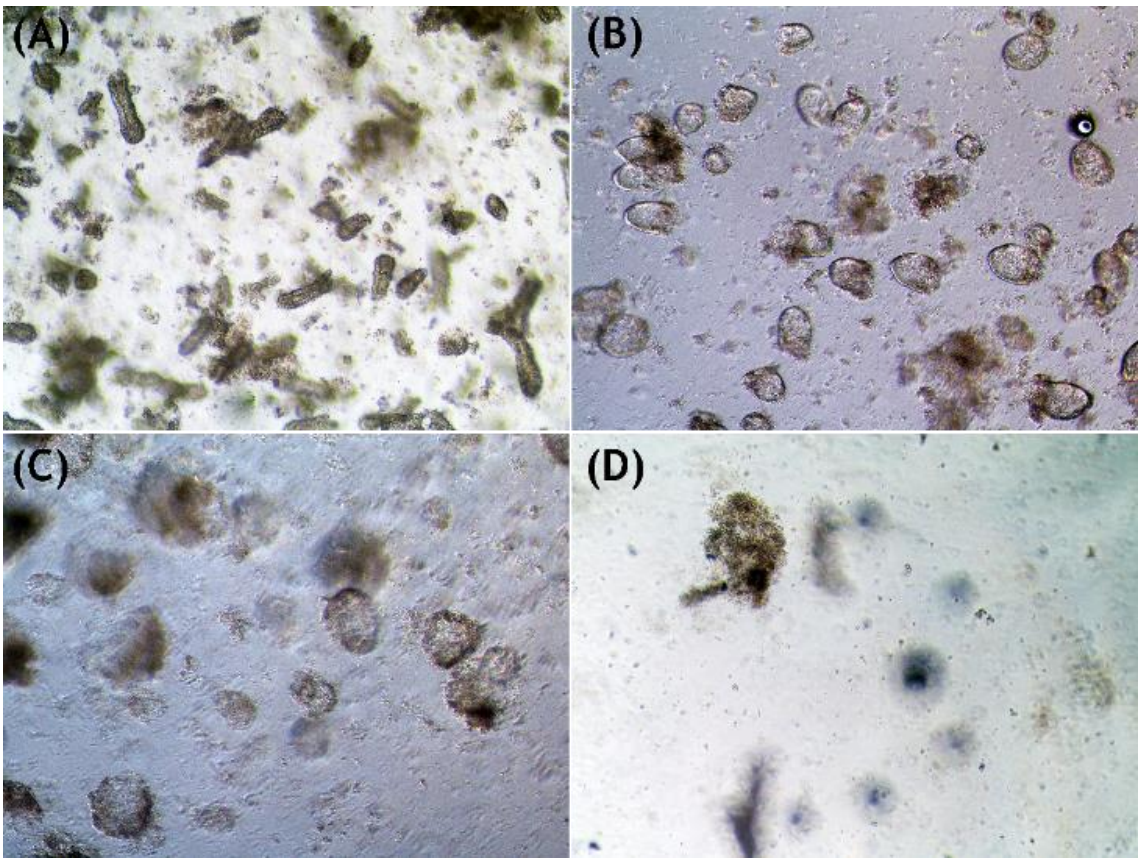

***Figure 22** – Optical microscopy images of organoid-like culture derived from ileum, maintained in culture for 7 days (A-C) and subcultured with lost of structure (D), 4x magnification.*

3.2.1. Conditioned media

HEK-293-Noggin (**Figure 23**) and L-wnt3a (**Figure 24**) cells were expanded in different selection media until reaching confluence and then grown on conditioning media. The final purpose was to harvest the resulting growth media as it contained important factors (Noggin and Wnt, respectively) for subsequent use in organoid cultures.

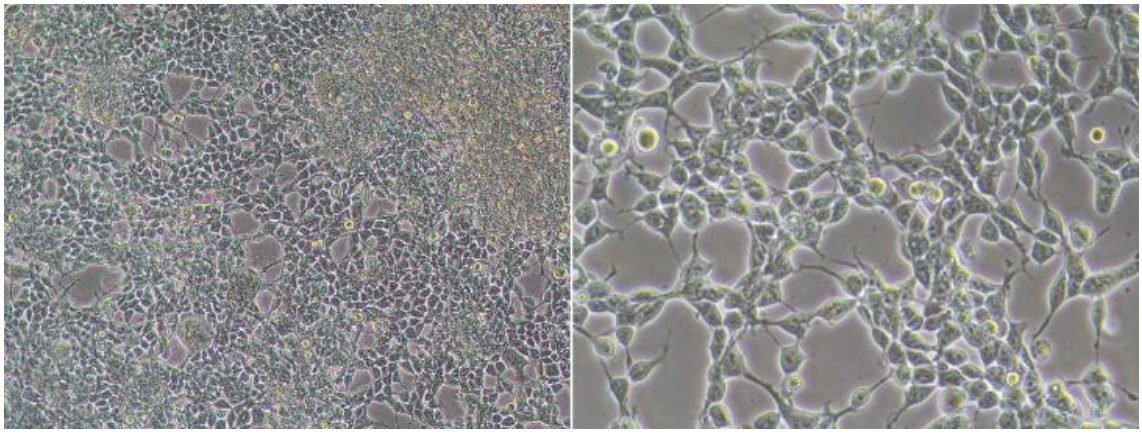

***Figure 23** - Optical microscopy images of HEK-293-Noggin cells at passages 11 (left panel, 10x magnification) and 12 (right panel, 20x magnification).*

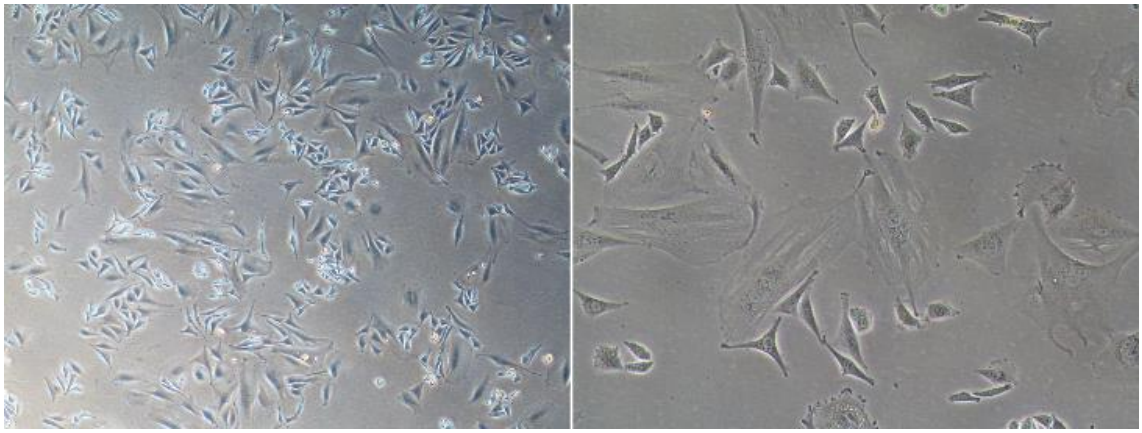

***Figure 24** - Optical microscopy images of L-wnt3a cells at passages 14 (left panel, 4x magnification) and 13 (right panel, 10x magnification).*

Chapter VI

Conclusions

This work showed the development of a gut-chip to recreate some *in vivo* characteristics of the human intestine, such as its three-dimensionality and flow dynamics, with the purpose of developing a model with increased physiological relevance. In fact, primary results showed that integrating continuous flow enabled cell proliferation and differentiation into an intestinal-like architecture.

The functional assay targeting P-gp inhibition demonstrated that both Verapamil and Green Tea function as inhibitors, considering the decrease in Rho123 P_{app} (BA) values. Importantly, green tea can be used as a natural P-gp inhibitor aiming to increase the bioavailability of orally administrated compounds, since intestinal absorption is limited by efflux transporters, such as BCRP and MRPs.

The P_{app} of Rho123 in the Gut-Chip was equivalent to the static cell culture inserts, validating the microfluidic device for intestinal absorption studies. Difficulties in sampling motivate further developments aiming to obtain an automated sampling system or an in-line measurement rig for improved performance. Further experiments including improved sampling strategies and other test solutions (*e.g.* green tea) will provide more information and allow for an accurate and comprehensive comparison between the static and dynamic models in use.

Human intestinal organoids were successfully obtained from primary intestinal cell isolation. The isolation protocol was optimised to achieve the growth of organoids, in particular regarding the sample processing time after collection. Although organoid-like structures started to develop one day after crypt culture, it was not possible to subculture them after 1 week. Therefore, changes in the protocol are being issued, including the use of a commercially available Expansion Media. However, this was not

addressed in scope of this dissertation and will be considered for future work within the research group.

After successfully culturing the organoids, the aim is to establish organoid-derived 2D monolayer cultures on-chip to increase the physiological relevance of the model. Thus, the recovery of intestinal crypts from distinct patients, may give rise to the development of personalized models of the intestine. Moreover, collecting tissue samples with different origins can elucidate some mechanisms of intestinal epithelium senescence with aging, or other gastrointestinal-related diseases.

Finally, a comprehensive comparison between the use of immortalized cell lines (Caco-2/HT29-MTX) and primary intestinal cell lines should be addressed by evaluating the physiological relevance of each cell model and their potential applications in assessing intestinal permeability.

Bibliography

Abdallah, H. M., Al-Abd, A. M., El-Dine, R. S., & El-Halawany, A. M. (2015). P-glycoprotein inhibitors of natural origin as potential tumor chemo-sensitizers: A review. In *Journal of Advanced Research* (Vol. 6, Issue 1, pp. 45–62). J Adv Res. https://doi.org/10.1016/j.jare.2014.11.008

Ampasavate, C., Sotanaphun, U., Phattanawasin, P., & Piyapolrungroj, N. (2010). Effects of Curcuma spp. on P-glycoprotein function. *Phytomedicine*, *17*(7), 506–512. https://doi.org/10.1016/j.phymed.2009.09.004

Anderle, P., Huang, Y., & Sadée, W. (2004). Intestinal membrane transport of drugs and nutrients: Genomics of membrane transporters using expression microarrays. *European Journal of Pharmaceutical Sciences*, *21*(1), 17–24. https://doi.org/10.1016/S0928-0987(03)00169-6

Ashammakhi, N., Nasiri, R., Barros, N. R. de, Tebon, P., Thakor, J., Goudie, M., Shamloo, A., Martin, M. G., & Khademhosseni, A. (2020). Gut-on-a-chip: Current progress and future opportunities. *Biomaterials*, *255*(November 2019). https://doi.org/10.1016/j.biomaterials.2020.120196

Bäckhed, F., Ley, R. E., Sonnenburg, J. L., Peterson, D. A., & Gordon, J. I. (2005). Host-bacterial mutualism in the human intestine. In *Science* (Vol. 307, Issue 5717). https://doi.org/10.1126/science.1104816

Beaurivage, C., Kanapeckaite, A., Loomans, C., Erdmann, K. S., Stallen, J., & Janssen, R. A. J. (2020). Development of a human primary gut-on-a-chip to model inflammatory processes. *Scientific Reports*, *10*(1). https://doi.org/10.1038/s41598-020-78359-2

Béduneau, A., Tempesta, C., Fimbel, S., Pellequer, Y., Jannin, V., Demarne, F., & Lamprecht, A. (2014). A tunable Caco-2/HT29-MTX co-culture model mimicking variable permeabilities of the human intestine obtained by an original seeding procedure. *European Journal of Pharmaceutics and Biopharmaceutics*, *87*(2). https://doi.org/10.1016/j.ejpb.2014.03.017

Bein, A., Shin, W., Jalili-Firoozinezhad, S., Park, M. H., Sontheimer-Phelps, A., Tovaglieri, A., Chalkiadaki, A., Kim, H. J., & Ingber, D. E. (2018). Microfluidic Organ-on-a-Chip Models of Human Intestine. *Cellular and Molecular Gastroenterology and Hepatology*, *5*(4), 659–668. https://doi.org/10.1016/j.jcmgh.2017.12.010

Bhatia, S. N., & Ingber, D. E. (2014). Microfluidic organs-on-chips. In *Nature Biotechnology* (Vol. 32, Issue 8, pp. 760–772). https://doi.org/10.1038/nbt.2989

Carsalade, B., Kant, R., Mukesh, R., Namita, P., & Vijay, K. J. (2012). Camellia Sinensis (Green Tea): A Review. *Global Journal of Pharmacology*, *6*(2), 52–59.

Choi, S. U., Park, S. H., Kim, K. H., Choi, E. J., Kim, S., Park, W. K., Zhang, Y. H., Kim, H. S., Jung, N. P., & Lee, C. O. (1998). The bisbenzylisoquinoline alkaloids, tetrandine and fangchinoline, enhance the cytotoxicity of multidrug resistance-related drugs via modulation of P-glycoprotein. *Anti-Cancer Drugs*, *9*(3), 255–261. https://doi.org/10.1097/00001813-199803000-00008

Creff, J., Malaquin, L., & Besson, A. (2021). In vitro models of intestinal epithelium: Toward bioengineered systems. *Journal of Tissue Engineering*, *12*. https://doi.org/10.1177/2041731420985202

Diehl, H. P., Wildey, A., Prasasty, V. D., & Siahaan, T. J. (2020). Organization of the intestinal mucosa and barriers to oral drug delivery. In *Nanotechnology for Oral Drug Delivery: From Concept to Applications* (pp. 7–25). Elsevier Inc. https://doi.org/10.1016/B978-0-12-818038-9.00002-8

Dubé, C. (2020). Duodenum Anatomy and Small Intestinal Development. In *Encyclopedia of Gastroenterology* (pp. 109–116). Academic Press. https://doi.org/10.1016/b978-0-12-801238-3.11335-2

Dutta, D., & Clevers, H. (2017). Organoid culture systems to study host–pathogen interactions. In *Current Opinion in Immunology* (Vol. 48, pp. 15–22). https://doi.org/10.1016/j.coi.2017.07.012

Dutton, J. S., Hinman, S. S., Kim, R., Wang, Y., & Allbritton, N. L. (2019). Primary Cell-Derived Intestinal Models: Recapitulating Physiology. *Trends in Biotechnology*, *37*(7), 744–760. https://doi.org/10.1016/j.tibtech.2018.12.001

Fatehullah, A., Tan, S. H., & Barker, N. (2016). Organoids as an in vitro model of human development and disease. In *Nature Cell Biology* (Vol. 18, Issue 3, pp. 246–254). https://doi.org/10.1038/ncb3312

Fernández-García, E., Carvajal-Lérida, I., & Pérez-Gálvez, A. (2009). In vitro bioaccessibility assessment as a prediction tool of nutritional efficiency. In *Nutrition Research* (Vol. 29, Issue 11, pp. 751–760). https://doi.org/10.1016/j.nutres.2009.09.016

Higgins, C. F., & Gottesman, M. M. (1992). Is the multidrug transporter a flippase? *Trends in Biochemical Sciences*, *17*(1), 18–21. https://doi.org/10.1016/0968-0004(92)90419-A

Hu, T., To, K. K. W., Wang, L., Zhang, L., Lu, L., Shen, J., Chan, R. L. Y., Li, M., Yeung, J. H. K., & Cho, C. H. (2014). Reversal of P-glycoprotein (P-gp) mediated multidrug resistance in colon cancer cells by cryptotanshinone and dihydrotanshinone of Salvia miltiorrhiza. *Phytomedicine*, *21*(11), 1264–1272. https://doi.org/10.1016/j.phymed.2014.06.013

Jalili-Firoozinezhad, S., Gazzaniga, F. S., Calamari, E. L., Camacho, D. M., Fadel, C. W., Bein, A., Swenor, B., Nestor, B., Cronce, M. J., Tovaglieri, A., Levy, O., Gregory, K. E., Breault, D. T., Cabral, J. M. S., Kasper, D. L., Novak, R., & Ingber, D. E. (2019). A complex human gut microbiome cultured in an anaerobic intestine-on-a-chip. *Nature Biomedical Engineering*, *3*(7), 520–531. https://doi.org/10.1038/s41551-019-0397-0

Juliano, R. L., & Ling, V. (1976). A surface glycoprotein modulating drug permeability in Chinese hamster ovary cell mutants. *Biochimica et Biophysica Acta (BBA) - Biomembranes*, *455*(1), 152–162. https://doi.org/10.1016/0005-2736(76)90160-7

Kasendra, M., Luc, R., Yin, J., Manatakis, D. V., Kulkarni, G., Lucchesi, C., Sliz, J., Apostolou, A., Sunuwar, L., Obrigewitch, J., Jang, K. J., Hamilton, G. A., Donowitz, M., & Karalis, K. (2020). Duodenum intestine-chip for preclinical drug assessment in a human relevant model. *ELife*, *9*. https://doi.org/10.7554/eLife.50135

Kasendra, M., Tovaglieri, A., Sontheimer-Phelps, A., Jalili-Firoozinezhad, S., Bein, A., Chalkiadaki, A., Scholl, W., Zhang, C., Rickner, H., Richmond, C. A., Li, H., Breault, D. T., & Ingber, D. E. (2018). Development of a primary human Small Intestine-on-a-Chip using biopsy-derived organoids. *Scientific Reports*, *8*(1), 1–14. https://doi.org/10.1038/s41598-018-21201-7

Kim, H. J., Huh, D., Hamilton, G., & Ingber, D. E. (2012). Human gut-on-a-chip inhabited by microbial flora that experiences intestinal peristalsis-like motions and flow. *Lab on a Chip*, *12*(12), 2165–2174. https://doi.org/10.1039/c2lc40074j

Kim, H. J., & Ingber, D. E. (2013). Gut-on-a-Chip microenvironment induces human intestinal cells to undergo villus differentiation. *Integrative Biology (United Kingdom)*, *5*(9), 1130–1140. https://doi.org/10.1039/c3ib40126j

Kim, H. J., Li, H., Collins, J. J., & Ingber, D. E. (2016). Contributions of microbiome and mechanical deformation to intestinal bacterial overgrowth and inflammation in a human gut-on-a-chip. *Proceedings of the National Academy of Sciences of the United States of America*, *113*(1), E7–E15. https://doi.org/10.1073/pnas.1522193112

Laksitorini, M., Prasasty, V., Kiptoo, P., & Siahaan, T. (2014). Pathways and progress in improving drug delivery through the intestinal mucosa and blood–brain barriers. *Pathways and Progress in Improving Drug Delivery through the Intestinal Mucosa and Blood–Brain Barriers*, *10*(5), 1143–1163. https://doi.org/10.4155/TDE.14.67

Langerholc, T., Maragkoudakis, P. A., Wollgast, J., Gradisnik, L., & Cencic, A. (2011). Novel and established intestinal cell line models - An indispensable tool in food science and nutrition. In *Trends in Food Science and Technology* (Vol. 22, Issue SUPPL. 1). https://doi.org/10.1016/j.tifs.2011.03.010

Lee, G., Joung, J. Y., Cho, J. H., Son, C. G., & Lee, N. (2018). Overcoming P-Glycoprotein-Mediated Multidrug Resistance in Colorectal Cancer: Potential Reversal Agents among Herbal Medicines. *Evidence-Based Complementary and Alternative Medicine*, *2018*. https://doi.org/10.1155/2018/3412074

Lee, J. S., Paull, K., Alvarez, M., Hose, C., Monks, A., Grever, M., Fojo, A. T., & Bates, S. E. (1994). Rhodamine efflux patterns predict P-glycoprotein substrates in the National Cancer Institute drug screen. *Molecular Pharmacology*, *46*(4), 627–638. https://citeseerx.ist.psu.edu/viewdoc/download?doi=10.1.1.854.168&rep=rep1&type=pdf

Lu, W. D., Qin, Y., Yang, C., Li, L., & Fu, Z. X. (2013). Effect of curcumin on human colon cancer multidrug resistance in vitro and in vivo. *Clinics*, *68*(5), 694–701. https://doi.org/10.6061/clinics/2013(05)18

Martins, E., Silva, V., Lemos, A., Palmeira, A., Puthongking, P., Sousa, E., Rocha-Pereira, C., Ghanem, C. I., Carmo, H., Remião, F., & Silva, R. (2019). Newly synthesized oxygenated xanthones as potential P-glycoprotein activators: In vitro, ex vivo, and in silico studies. *Molecules*, *24*(4). https://doi.org/10.3390/molecules24040707

Ordóñez-Morán, P. (Ed.). (2020). *Intestinal Stem Cells* (Vol. 2171). Springer US. https://doi.org/10.1007/978-1-0716-0747-3

Rahman, S., Ghiboub, M., Donkers, J. M., van de Steeg, E., van Tol, E. A. F., Hakvoort, T. B. M., & de Jonge, W. J. (2021). The progress of intestinal epithelial models from cell lines to gut-on-chip. In *International Journal of Molecular Sciences* (Vol. 22, Issue 24). https://doi.org/10.3390/ijms222413472

Ramadan, Q., & Jing, L. (2016). Characterization of tight junction disruption and immune response modulation in a miniaturized Caco-2/U937 coculture-based in vitro model of the human intestinal barrier. *Biomedical Microdevices*, *18*(1), 1–9. https://doi.org/10.1007/s10544-016-0035-5

Rocha-Pereira, C., Ghanem, C. I., Silva, R., Casanova, A. G., Duarte-Araújo, M.,

Gonçalves-Monteiro, S., Sousa, E., Bastos, M. de L., & Remião, F. (2020). P-glycoprotein activation by 1-(propan-2-ylamino)-4-propoxy-9H-thioxanthen-9-one (TX5) in rat distal ileum: ex vivo and in vivo studies. *Toxicology and Applied Pharmacology*, *386*(September 2019), 114832. https://doi.org/10.1016/j.taap.2019.114832

Round, J. L., & Mazmanian, S. K. (2009). The gut microbiota shapes intestinal immune responses during health and disease. In *Nature Reviews Immunology* (Vol. 9, Issue 5). https://doi.org/10.1038/nri2515

Sadabad, M. S., Von Martels, J. Z. H., Khan, M. T., Blokzijl, T., Paglia, G., Dijkstra, G., Harmsen, H. J. M., & Faber, K. N. (2015). A simple coculture system shows mutualism between anaerobic faecalibacteria and epithelial Caco-2 cells. *Scientific Reports*, *5*. https://doi.org/10.1038/srep17906

Sato, T., Stange, D. E., Ferrante, M., Vries, R. G. J., Van Es, J. H., Van Den Brink, S., Van Houdt, W. J., Pronk, A., Van Gorp, J., Siersema, P. D., & Clevers, H. (2011). Long-term expansion of epithelial organoids from human colon, adenoma, adenocarcinoma, and Barrett's epithelium. *Gastroenterology*, *141*(5), 1762–1772. https://doi.org/10.1053/j.gastro.2011.07.050

Sato, T., Vries, R. G., Snippert, H. J., Van De Wetering, M., Barker, N., Stange, D. E., Van Es, J. H., Abo, A., Kujala, P., Peters, P. J., & Clevers, H. (2009). Single Lgr5 stem cells build crypt-villus structures in vitro without a mesenchymal niche. *Nature*, *459*(7244), 262–265. https://doi.org/10.1038/nature07935

Seelig, A. (2020). P-Glycoprotein: One Mechanism, Many Tasks and the Consequences for Pharmacotherapy of Cancers. *Frontiers in Oncology*, *10*, 576559. https://doi.org/10.3389/fonc.2020.576559

Sharom, Frances J. (2011). The P-glycoprotein multidrug transporter. *Essays in Biochemistry*, *50*(1), 161–178. https://doi.org/10.1042/BSE0500161

Sharom, Frances Jane. (2014). Complex interplay between the P-glycoprotein multidrug efflux pump and the membrane: Its role in modulating protein function. *Frontiers in Oncology*, *4 MAR*. https://doi.org/10.3389/FONC.2014.00041

Shim, K. Y., Lee, D., Han, J., Nguyen, N. T., Park, S., & Sung, J. H. (2017). Microfluidic gut-on-a-chip with three-dimensional villi structure. *Biomedical Microdevices*, *19*(2). https://doi.org/10.1007/s10544-017-0179-y

Silva, R., Vilas-Boas, V., Carmo, H., Dinis-Oliveira, R. J., Carvalho, F., De Lourdes Bastos, M., & Remião, F. (2015). Modulation of P-glycoprotein efflux pump: Induction and activation as a therapeutic strategy. In *Pharmacology and Therapeutics* (Vol. 149, pp. 1–123). https://doi.org/10.1016/j.pharmthera.2014.11.013

Steffansen, B., Nielsen, C. U., Brodin, B., Eriksson, A. H., Andersen, R., & Frokjaer, S. (2004). Intestinal solute carriers: An overview of trends and strategies for improving oral drug absorption. *European Journal of Pharmaceutical Sciences*, *21*(1), 3–16. https://doi.org/10.1016/J.EJPS.2003.10.010

Tamura, H. O., & Matsui, M. (2000). Inhibitory Effects of Green Tea and Grape Juice on the Phenol Sulfotransferase Activity of Mouse Intestines and Human Colon Carcinoma Cell Line, Caco-2. *Biological and Pharmaceutical Bulletin*, *23*(6), 695–699. https://doi.org/10.1248/BPB.23.695

Thompson, C. A., DeLaForest, A., & Battle, M. A. (2018). Patterning the gastrointestinal epithelium to confer regional-specific functions. *Developmental*

Biology, *435*(2), 97–108. https://doi.org/10.1016/J.YDBIO.2018.01.006

Troutman, M. D., & Thakker, D. R. (2003). *Rhodamine 123 Requires Carrier-Mediated Influx for Its Activity as a P-Glycoprotein Substrate in Caco-2 Cells*.

Westerhout, J., Van De Steeg, E., Grossouw, D., Zeijdner, E. E., Krul, C. A. M., Verwei, M., & Wortelboer, H. M. (2014). A new approach to predict human intestinal absorption using porcine intestinal tissue and biorelevant matrices. *European Journal of Pharmaceutical Sciences*, *63*, 167–177. https://doi.org/10.1016/j.ejps.2014.07.003

Williamson, I. A., Arnold, J. W., Samsa, L. A., Gaynor, L., DiSalvo, M., Cocchiaro, J. L., Carroll, I., Azcarate-Peril, M. A., Rawls, J. F., Allbritton, N. L., & Magness, S. T. (2018). A High-Throughput Organoid Microinjection Platform to Study Gastrointestinal Microbiota and Luminal Physiology. *CMGH*, *6*(3). https://doi.org/10.1016/j.jcmgh.2018.05.004

Workman, M. J., Gleeson, J. P., Troisi, E. J., Estrada, H. Q., Kerns, S. J., Hinojosa, C. D., Hamilton, G. A., Targan, S. R., Svendsen, C. N., & Barrett, R. J. (2018). Enhanced Utilization of Induced Pluripotent Stem Cell–Derived Human Intestinal Organoids Using Microengineered Chips. *Cmgh*, *5*(4), 669-677.e2. https://doi.org/10.1016/j.jcmgh.2017.12.008

Zhang, L., Chow, M. S. S., & Zuo, Z. (2006). Effect of the co-occurring components from green tea on the intestinal absorption and disposition of green tea polyphenols in Caco-2 monolayer model. *JPP*, *58*, 37–44. https://doi.org/10.1211/jpp.58.1.0005

Zhang, L., Zheng, Y., Chow, M. S. S., & Zuo, Z. (2004). Investigation of intestinal absorption and disposition of green tea catechins by Caco-2 monolayer model. *International Journal of Pharmaceutics*, *287*(1–2), 1–12. https://doi.org/10.1016/j.ijpharm.2004.08.020